Final Report

on

Stabilized CO_2 Gas Laser

(1 December 1966 - 30 January 1968)

Contract No. NAS5-10309

Prepared by

Sylvania Electronic Systems
Western Division
Mountain View, California

for

Goddard Space Flight Center
Greenbelt, Maryland

Final Report

on

Stabilized CO_2 Gas Laser

(1 December 1966 - 30 January 1968)

Contract No. NAS5-10309

Goddard Space Flight Center
Contracting Officer: A. L. Essex
Technical Monitor: Nelson McAvoy

Prepared by

Sylvania Electronic Systems
Western Division
Mountain View, California
Project Manager: R. S. Reynolds

Approved by

M. B. Fisher, Manager
Electro-Optic Devices Department

B. J. McMurtry, Director
Electro-Optics Organization

for

Goddard Space Flight Center
Greenbelt, Maryland

FOREWORD

This report is the Final Engineering Report summarizing the work performed under NASA Contract NAS5-10309 entitled "Stabilized CO_2 Gas Laser," covering the period 1 December 1966 to 30 January 1968. This report was prepared by the Electro-Optics Organization of Sylvania Electronics Systems - Western Division, Mountain View, California. It describes work performed in the Electro-Optic Devices Department, headed by Mr. Mahlon B. Fisher. Mr. Richard S. Reynolds is the principal investigator on the program. Dr. J. D. Foster also contributed to this report.

All the work performed under this contract was administered by the Optics Branch, NASA-Goddard Space Flight Center, Greenbelt, Maryland. Mr. N. McAvoy is the principal technical representative for the Optics Branch.

ABSTRACT

This report describes the results of a program directed toward the design and development of a CO_2 laser capable of high power at a single frequency, highly stabilized on the short term. This laser has been developed for use in long range communications systems and is capable of operating in any position without affecting the operating characteristics.

The laser utilizes a master-oscillator, power-amplifier to achieve high power simultaneously with high stability and is capable of providing up to 38 watts of single-frequency light in the TEM_{00q} mode. A temperature-controlled oscillator provides 5 watts of power at a single wavelength at 10.6 microns for an active plasma length of 50 cm. The amplifier utilizes a folded structure with a total optical path of about 7 meters. DC excitation was used.

A second oscillator, identical to the first, was used to obtain relative frequency stability information by heterodyne techniques. Long-term stability, as determined by the thermal environment was about $\pm$ 3 parts in 10^7. The short-term stability varied between 5 parts in 10^{11} and 1 part in 10^9 over a 10 ms time interval. The short-term frequency stability depends strongly on the laser acoustical environment.

Experimental results are also presented on the effects of RF excitation, laser bore size and gas mixture on the laser output.

TABLE OF CONTENTS

LIST OF FIGURES

LIST OF FIGURES

1.0 INTRODUCTION

Since the discovery of the CO_2 laser in 1964, much interest has been generated for its use in applications involving communications and telemetry. The desirable combination of high efficiency with a high power output capability is coupled with an operating wavelength (10.6 microns) which occurs in an atmospheric "transmission window". Also it appears that single frequency operation of the CO_2 laser is possible even at high power levels allowing the development of certain types of communication systems which could not be fully utilized with other types of lasers. With these major advantages, along with several other minor advantages associated with operation in the infrared (large coherence area, lower quantum noise, etc.), the necessity for the development of components suitable for operation in a sophisticated 10.6-micron system has become apparent.

This program has been concerned with the development of a suitable CO_2 laser transmitter capable of being used in an earth-to satellite -- to earth communication link. Specifically, the program involves the development of a laser which is capable of operating at a power level exceeding 20 watts, with the output linearly polarized and with the power contained in a single frequency corresponding to a wavelength of about 10.6 microns. The laser is to be used in a homodyne mode where a portion of the output beam is tapped and used as a local oscillator for the returned beam from the satellite. In this mode of operation good frequency stability of the laser is required during the time of flight (in this case 10 ms) of the optical beam to the satellite and back. Slow drifts in the output frequency of the laser will not be noticed in this type of system, therefore only moderate long-term stability is required.

Other important factors in the development of this laser are weight and convenience of operation since the laser will be installed on a rotating telescope remotely located from the telescope control room. The capability of maintaining the operating characteristics of the laser is essential even as the laser is rotated and tilted.

To achieve these goals, a master-oscillator, power amplifier approach was taken utilizing sealed-off plasma tubes with Brewster angle windows. It was determined early in the program that active electronic stabilization would not be necessary to achieve the required long-and short-term frequency stabilities and that close attention to the details of mechanical and thermal design would provide the desired results. A unique invar-aluminum laser cavity configuration was utilized to provide an oscillator with appropriate dimensions and configuration to provide the required stabilities. A lightweight amplifier, folded to reduce overall length, was then used to boost the oscillator power without adding any significant noise or instabilities to the beam.

The most satisfactory technique for measuring the frequency stability of a laser is to use heterodyne techniques even though only relative frequency stability is obtained this way. A second laser oscillator was constructed to use as a local oscillator for the frequency stability measurements. This laser was constructed identically to the first so that each laser could be considered to contribute equally to any instabilities which could be measured.

Section 2.0 describes the laser system in detail and discusses the mechanical and electrical design of both the high power and low power lasers, section 3.0 lists the various experiments and studies performed during the program, section 4.0 contains the description of any new technological developments during the program, section 5.0 contains a statement on materials processing during the program and section 6.0 summarizes the results of the program. Section 7.0 contains the references used in this report.

2.0 TECHNICAL APPROACH

2.1 General

The basic system approach we have used toward establishing a high-power, high-stability CO_2 laser is diagramed in Figure 1. To achieve the simultaneous requirements of high power and high-frequency stability, a master oscillator-power amplifier approach has been taken. The high gain on the CO_2 laser transition makes this approach feasible. The oscillator length (and therefore power) was limited by vibrational effects in the mechanical structure, and the overall weight of the unit. For longer structures, which would be capable of delivering higher powers, the necessary cross-sectional area becomes large for good vibration resistance and the weight grows rapidly. The design weight of the laser oscillator was set at about 50 lbs resulting in an external cavity length of about 92 cm. With an active length of about 50 cm the oscillator is capable of delivering about 4 to 5 watts of single-mode power.

The amplifiers which follow the laser oscillator must be long enough to provide for a power gain of about 4 to 5. Since the amplifiers are not part of a resonant cavity, lightweight supports are all that are required in the mounting of the amplifiers.

The system in which the laser will be used utilizes polarization sensitive optics; and, therefore, to maintain an overall high transmission factor for the system, the laser has been designed to utilize Brewster angle windows.

Wavelength selection is to be obtained by length tuning the laser cavity. It has been found that the laser will oscillate nearly simultaneously in several laser transitions, each corresponding to different output wavelength. However, by carefully adjusting the optical length of the laser cavity, stable

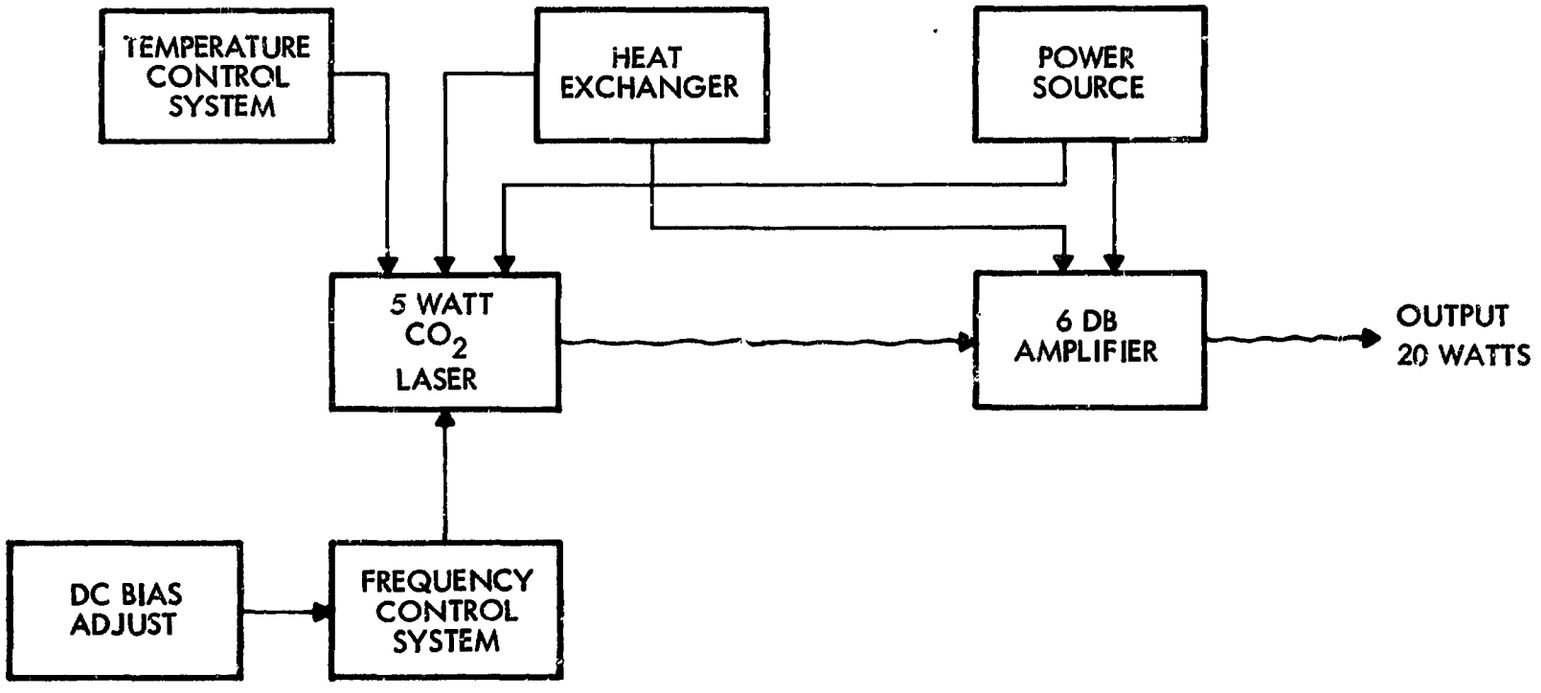

Figure 1. System Diagram of High-Power, Frequency-Stabilized CO_2 Laser.

single-wavelength operation can be obtained in any one of the several high gain lines. Also by controlling and maintaining the temperature of the laser cavity, the laser can be turned on and off and still operate at a preselected wavelength.

The primary purpose of the dc bias adjust, shown in Figure 1, is to allow the selection of the operating wavelength. This adjustment will control the cavity mirror separation by changing the bias voltage applied to a piezoelectric transducer on which the back laser mirror is attached. Once the proper bias voltage is selected, the temperature control system will control the temperature of the laser cavity so that the laser operating frequency will always lie within the selected CO_2 Doppler line. As long as the temperature control system is operating properly, the absolute optical length of the cavity will allow the laser to always operate at a single preselected wavelength. The temperature control system is capable of maintaining the cavity temperature to an accuracy of about $\pm$ 0.1°C. Higher accuracies are limited by the presence of the active laser installed inside the laser cavity. In order for the laser to operate at maximum power, the plasma tubes must be cooled by a low-velocity liquid cooling system. A self-contained heat exchanger has been used for this purpose.

The final lasers and amplifiers utilize dc excitation although RF excitation was used during the early portions of the program. The initial interest in using RF excitation was generated by the excellent CO_2 laser lifetime data from French* experimenters who were using RF excitation techniques. Their results were substantially better than that obtained with dc excitation (at that time). Subsequently we found nearly simultaneously that the maximum single mode power from the laser was substantially increased when dc excitation was used instead of RF excitation and that reasonable lifetimes were beginning to be observed for some designs of dc operated tubes. Before the switch to dc operation was completed, much valuable information was obtained on RF excited tubes and is included in later sections.

---

*Laboratoire de Physique, de la Societe Anonymite de Telecommunications, 41 rue Cantagrel, Paris, 13e.

2.2 Mechanical Design

2.2.1 Vibration Control

Under normal environments, the laser output frequency, with its very narrow instantaneous spectral width wanders in frequency due to small changes in the relative position of the laser mirrors. The relative frequency change of the laser associated with this length change caused by either thermal or vibrational effects is given by

$$\frac{df}{f} = -\frac{dL}{L}$$

where f is the laser operating frequency and L is the separation of the laser mirrors. Over short time periods the wanderings of the output frequency may be averaged by the measuring instruments used to detect these frequency shifts and the extent of the vibrational instabilities then are related to the measured spectral width of the laser beam.

The lower limit to the extent of the frequency wandering can be predicted[1] from the thermal excitation of the lowest frequency longitudinal mode of the laser cavity structure. For the type of cavities used on the stabilized CO_2 laser, the fundamental value for the vibration frequency stability is about

$$\left(\frac{\Delta f}{f}\right)_{\text{thermal vibration}} = 2 \times 10^{-15},$$

small compared to the stabilities achieved in normal laboratory environments.

If acoustical and mechanical vibration inputs to the structure have significant power at longitudinal mode frequencies of the structure, the magnitude of the wandering of the laser frequency will be increased. In addition, real laser structures may have elements with beam-like or plate-like geometries. Beams and plates have transverse vibration modes which may occur at quite low frequencies. Also, the joints between elements may

have low-frequency modes. If any of these additional vibration modes occur at frequencies included in the power spectra of the acoustical and mechanical vibration inputs, the frequency wandering of the laser will be even further increased.

In order for a structure to be stable against vibration, it is necessary that the mechanical resonances of the structure not be at frequencies within the main power spectrum of acoustical and mechanical vibration noise inputs.

Acoustical noise and mechanical vibration noise are actually identical quantities, but we will define them as two separate noise sources. Acoustic noise will be defined as noise energy transferred as sound waves through the air, and mechanical vibration noise will be defined as noise transferred through the structural mounting.

The main power spectrum of both acoustic and mechanical vibration noise is at low frequencies. The peak of the acoustic spectrum usually occurs at less than 500 Hz. The fact that most of the noise power spectrum for vibrational excitation occurs at low frequencies, together with the fact that high frequency noise is easier to isolate from a structure than is low frequency noise, dictates that the CO_2 laser structure should be designed to make the structural frequency resonances as high as can be achieved.

The frequency of the lowest longitudinal resonance of a laser cavity structure is determined by the effective cavity length. This frequency is given by the equation

$$f_{L\nu} = \frac{C_s}{2L}$$

where C_s is the velocity of sound in the structure, and L is the structure length.

In choosing a length for the CO_2 laser, one must make a trade-off between high longitudinal mode frequency and stiffness against distortion on the one hand and high output power on the other. Assuming a structure made of invar for thermal stability reasons, Table I shows the lowest longitudinal frequency for various cavity lengths.

Table I. Lowest Longitudinal Mode Frequencies in Invar Laser Cavities

Cavity Length	Frequency
2 m	1.2 kHz
1 m	2.5 kHz
50 cm	5.0 kHz
20 cm	12 kHz
10 cm	25 kHz

It is most desirable to keep $f_{L\nu}$ as large as possible to aid in acoustic isolation from the outside environment. At frequencies substantially below $f_{L\nu}$, the laser mirrors will oscillate in phase when excited by acoustical energy, and there will be no net change in the optical length of the cavity (and, therefore, no frequency change in the laser output). However, at $f_{L\nu}$, the mirrors move in opposition, and the laser frequency excursion is maximum. In general, acoustical-dampening materials, such as foam, laminate structures, etc., all attenuate acoustical energy more efficiently at the higher frequencies. Their attentuation characteristics are rather poor at very low frequencies. For this reason, a major effort in the design of the cavity has been placed on maintaining as high a lowest-order resonant frequency as possible for the chosen cavity length.

A nominal 1 m long total cavity length was chosen for this program as being able to provide fairly substantial output power (about 5 watt single frequency) while still maintaining fairly high lowest-order resonant frequencies in the range where substantial vibrational damping can be applied.

The design of the remaining structure was then chosen to keep from lowering the basic first resonance. The individual elements of the structure

were chosen with geometries and methods of support (boundary conditions) such that they do not have low frequency transverse resonances. The joints were also designed so that they do not have any low frequency resonances. Especially critical are the joints perpendicular to the cavity length. One particularly good design for these joints is to use large contact areas under compressional stress. The spring constant of the joint will then be high. Designs with joints using only the spring force of a few screws to connect significant masses must be avoided. Figure 2a shows a photograph of one of the oscillator cavities, and Figure 2b is an assembly drawing of the unit.

The cavity consists of a rigid channel-shaped structure with the laser tube mounted in the channel and the mirror mounts clamped to the ends. The channel-shaped structure was chosen because of its high resistance to bending deformation. When the lid is attached and the fourth side of the structure closed, the resistance to bending is almost identical to a cylindrical structure (optimum for resistance to bending) of similar cross-sectional dimensions. However, the rectangular structure allows much easier access to the cavity.

In order to conserve weight, but still maintain the required thermal characteristics, the channel-shaped cavity was constructed primarily from aluminum with invar rods embedded in the aluminum. The four invar rods, located at each corner of the channel, serve as mounting points for the mirror assemblies. The rods are potted into the aluminum frame so as to provide an intimate contact between the invar and the rigid aluminum structure.

Out of several lightweight structural materials, aluminum was chosen because of its relatively high velocity of sound factor. It is almost identical to the invar rods at about 5000 meters per second[2]. For the 92-cm long cavity length finally chosen, this velocity factor results in a calculated lowest longitudinal cavity resonance of about 2700 cps.

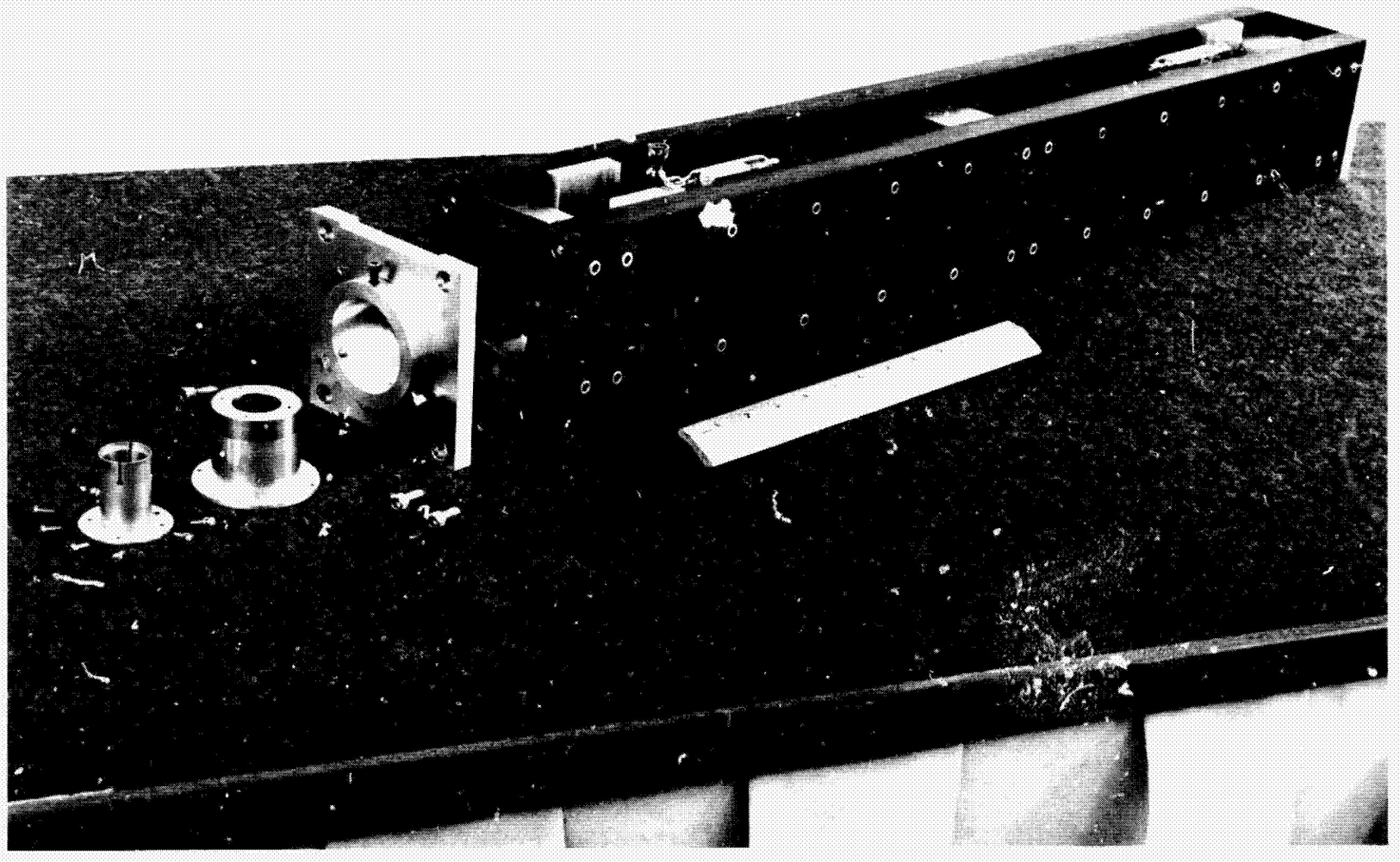

Figure 2a. Photograph of CO_2 Laser Cavity Structure.

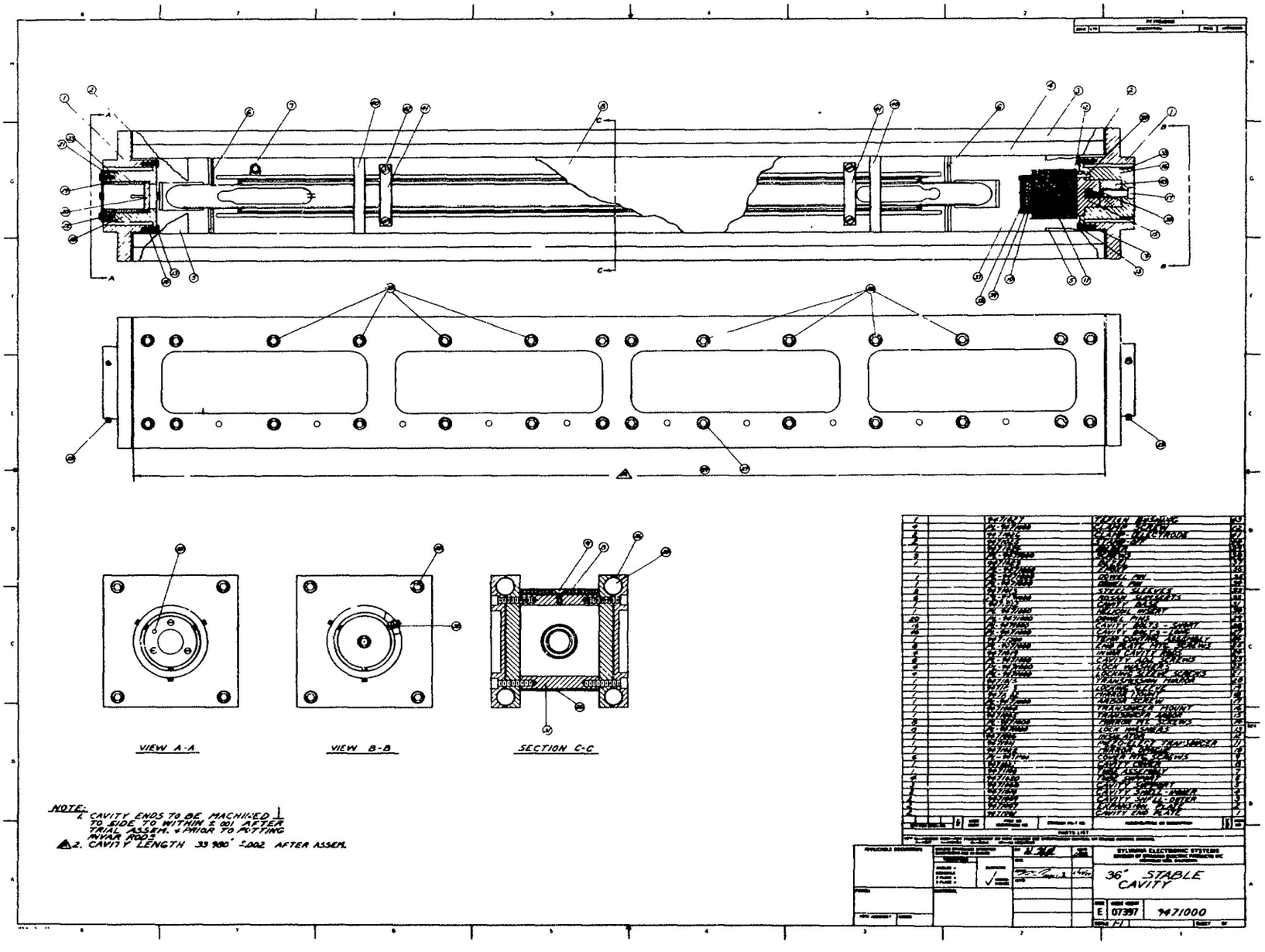

Figure 2b. Assembly Drawing of Stabilized CO_2 Laser Cavity

To remove the problems associated with weak spring-type controls, the mirror holders have been ruggedly designed. As can be seen in Figure 2, the mirrors can be adjusted in angle by distortion of the metal flange holding the mirror assembly. As the mirrors are being adjusted into their final position, the adjustment screws clamp the mirror holder tightly so that no inadvertent movement is possible. The mirror holder has been keyed so that mirrors can be removed and replaced without causing misalignment. The invar rods to which the mirror holders are tightly bolted are slightly longer than the aluminum cavity structure so the mirror mounts do not contact the aluminum (see next section on thermal control).

The laser tube has been mounted in the cavity with thin discs which provide good transverse stability while offering high impedance to vibrations which may be coupled to the cavity by the flowing coolant around the laser tube.

To further reduce the intensity of air born acoustic waves reaching the laser oscillator, the entire inside covers and base of the laser enclosure are covered with several layers of type Y-9052 industrial vibration damping material made by 3 M Company. This material is a pressure-sensitive, specially compounded polyurethane acoustic damping foam with an aluminum foil paper laminant constraining layer backing. The laminant structure is especially effective for vibration isolation and it also serves as an effective thermal shield to help maintain a uniform and controllable temperature within the laser enclosure.

2.2.2 Thermal Control

Although the requirement for high-frequency stability is only applicable for relatively short periods of time, the laser must be stable enough to operate continuously within the central portion of the CO_2 Doppler gain curve. This is necessary to ensure constant power and single wavelength operation.

The expected Doppler linewidth $\Delta\nu_D$ of any laser gas can be estimated[3] from the relationship

$$\Delta\nu_D = \frac{2\sqrt{2\ \ell n\ 2}}{\lambda} \sqrt{\frac{k\ T_{mol}}{M}}$$

where M is the molecular mass, and T_{mol} is the molecular temperature of the discharge, k is Boltzmann's constant (1.3×10^{-23} joules/^{o}C), and λ is the wavelength. For the CO_2 laser $\Delta\nu_D \approx 50$ MHz.

The degree of length stabilization required to maintain continuous single-frequency output with good power stability can be easily calculated. Assume that the maximum drift in frequency from the center of the Doppler gain curve can be only about 10% in order to obtain good power stability. Then the relative change in cavity length is

$$\left|\frac{\Delta L}{L}\right|_{total} = \frac{(\Delta f)}{f}$$

$$= \frac{(.1)\ 50\ \text{MHz}}{3 \times 10^{13}\ \text{Hz}} = 1.7 \times 10^{-7}$$

where L is the cavity length and f is the laser frequency. The degree of thermal stabilization required for the cavity structure can then be obtained since

$$\frac{\Delta L}{L} = \alpha\Delta T$$

where α is the thermal coefficient of expansion of the cavity material and ΔT is the total variation in cavity temperature with time.

Table II

Coefficient of Thermal Expansion
of Several Structural Materials

Material	α (per degree C)
Aluminum	25.5×10^{-6}
Copper	16.8
Glass	~ 8.5
Iron, Steel	10.0 - 12.0
Magnesium	26.0
Invar	0.90
Quartz (fused)	0.42
Special Glass and Cellular Ceramics	~ 0.10

Using the standard techniques of proportional temperature control, the expected realizable limit on ΔT is about $\pm$ 0.1°C for the configuration of the laser cavity, expected thermal load and environmental variations. With the above value of $\Delta L/L$, the required value of α is

$$\alpha_{required} = \frac{1.7 \times 10^{-7}}{0.1^{\circ}C}$$

$$= 1.7 \times 10^{-6}/^{\circ}C$$

Table II lists a few materials which could be used for a cavity structure along with their coefficient of thermal expansion. Because of its ease of machining and low expansion coefficient, invar was chosen as the primary thermal material.

The method of attachment of the invar rods to the aluminum channel-shaped structure is extremely critical. Rigid bonding, which would be most desirable from a resistance to bending viewpoint, would not be satisfactory from a thermal viewpoint since the aluminum will pull the invar as the temperature changes. The best compromise will be obtained by using a bonding material whose shear modulus of elasticity is just low enough that insignificant pulling of the invar by the aluminum will occur. The following is an analysis which was performed to help determine the appropriate bonding material.

Refering to Figure 3a, assume that the aluminum and the invar have both thermal and elastic deformations, but the epoxy has only elastic deformation. This assumption greatly simplifies the calculations and, as can be seen at the end of the analysis, this assumption is quite good.

From geometry, the differential thermal (T) expansion between the invar and the aluminum must equal the sum of the elastic (E) deformations in the three materials.

$$(\Delta L_{Al})_T - (\Delta L_{In})_T = (\Delta L_{In})_E + (\Delta L_{Al})_E + (\Delta L_{Ep})_E \qquad (1)$$

The total expansion of the invar is the quantity of interest. It is given by

$$(\Delta L_{In}) = (\Delta L_{In})_T + (\Delta L_{In})_E \qquad (2)$$

and to obtain (ΔL_{In}) we need to determine each of the individual deformations. For the case when $L \approx L_{In} \approx L_{Ep} \approx L_{Al}$

$$(\Delta L_{In})_1 = \alpha_{In} \; L \; \Delta \; T \qquad (3)$$

and $$(\Delta L_{Al})_T = \alpha_{Al} \; L \; \Delta \; T \qquad (4)$$

where α is the coefficient of thermal expansion and ΔT is the temperature rise of the material.

Considering the elastic deformation of the invar, the differential expansion between the aluminum and the invar will produce a shear stress in the epoxy which will increase linearly from the center of the structure to the ends. This stress can be expressed as a one dimensional distributed shear force, s, with dimensions of lb/in. The force will, of course, be assumed to act uniformly over the circumference of the invar at each position as depicted in Figure 3b.

Refering to the free body diagram in Figure 3b, the force acting on the invar at position x can be written as

$$P_x = \frac{1}{2} s_m \frac{L}{2} - \frac{1}{2} s_x x$$

$$= \frac{1}{2} \frac{s_m L}{2} - \frac{2 s_m x^2}{L}$$

and the elastic deformation $\Delta(dx)$ due to this force on an incremental length (dx) at x is given by

$$\Delta(dx) = \frac{P_x \, dx}{A_{In} E_{In}}$$

where A_{In} is the cross-sectional area of the invar and E_{In} is the modulus of elasticity of invar.

The total deformation for one half the length of invar will be the integral of the incremental values, and the total deformation will be twice the integral.

$$(\Delta L_{In})_E = 2 \int_0^{L/2} \frac{P_x \, dx}{A_{In} E_{In}}$$

$$(\Delta L_{In})_E = \frac{s_m L^2}{6 A_{In} E_{In}} \qquad (5)$$

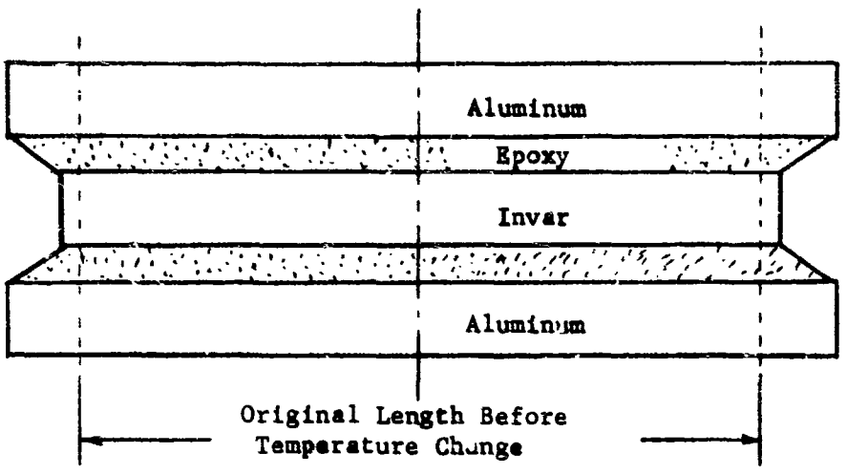

Figure 3a. Diagram of Aluminum Structure Holding Invar Rod with Epoxy

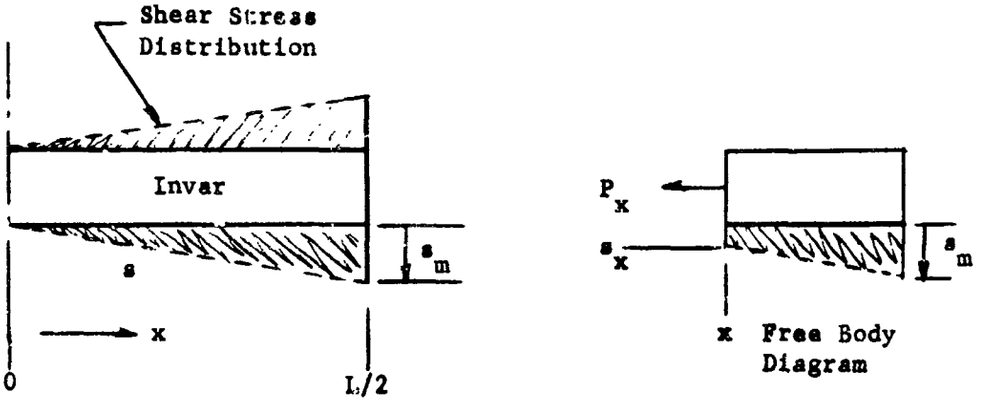

Figure 3b. Invar Rod with Distributed Stress

Similarly for the aluminum

$$(\Delta L_{Al})_E = \frac{s_m L^2}{6 A_{Al} E_{Al}} \tag{6}$$

Now to find the elastic deformation of the epoxy, consider an elemental ring of epoxy at position x with length dx. A cross section of this ring is shown below. Again the shear force is considered to be uniformly distributed from the center to each end of the epoxy joint and to act uniformly over the ring of epoxy.

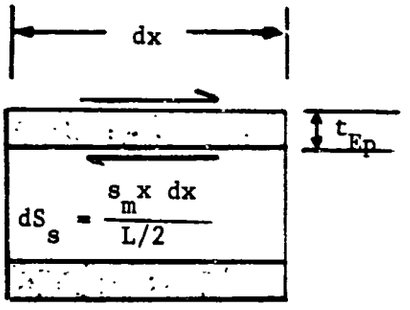

The deformation across the epoxy due to the shear strain at position x is then

$$\Delta(dx) = \frac{t_{Ep}\ dS_x}{C\ G_{Ep}\ dx} = \frac{2 s_m\ x\ t_{Ep}}{L\ C\ G_{Ep}}$$

where C is the circumference of the epoxy ring and G_{Ep} is the shear modulus of elasticity of the epoxy will be twice that at one end.

Since the area of the epoxy A_{Ep}, can be written $A_{Ep} = LC$ we can write for the maximum deformation which occurs at $x=L$ for the entire rod

$$(\Delta L_{Ep})_E = \frac{2\ s_m\ L\ t_{Ep}}{A_{Ep}\ G_{Ep}} \tag{7}$$

We now have all the relationships necessary to solve for ΔL_{In}. Substituting (3), (4), (5), (6) and (7) into equation (1) and solving for $s_m L$ we get

$$s_m L = \frac{(\alpha_{Al} - \alpha_{In})\, L\, \Delta\, T}{\frac{L}{6\, A_{In}\, E_{In}} + \frac{L}{6\, A_{Al}\, E_{Al}} + \frac{2\, t_{Ep}}{A_{Ep}\, G_{Ep}}} \tag{8}$$

combining equation (8) with (3), (5) and (2) and arranging the terms, we get, finally

$$\boxed{\frac{1}{\Delta T}\left(\frac{\Delta L}{L}\right)_{In} = \alpha_{In} + \frac{(\alpha_{Al} - \alpha_{In})}{1 + \frac{A_{In}\, E_{In}}{A_{Al}\, E_{Al}} + 12\, \frac{t_{Ep}}{L}\, \frac{A_{In}\, E_{In}}{A_{Ep}\, G_{Ep}}}} \tag{9}$$

which is the effective coefficient of expansion of the invar as it is pulled by the aluminum through the strength of the epoxy joint.

From a vibration viewpoint, it is most desirable to have the invar very tightly coupled to the aluminum structure. The rigidity and mass of the aluminum would tend to keep the resonant frequency of the overall mirror structure high. However, as seen from equation (9), when G_{Ep} is very large, the effective coefficient of expansion of the cavity approaches that of aluminum, which in this case would not be tolerable.

As an estimate of the magnitude of this effect, the following values apply:

$\alpha_{In} = 1 \times 10^{-6}/^{\circ}C$

$E_{In} = 27 \times 10^{6}$ psi

$A_{In} = 0.614$ in^2

$L = 39.4$ inches

$\alpha_{Al} = 22 \times 10^{-6}/^{\circ}C$

$E_{Al} = 10.5 \times 10^{6}$ psi

$A_{Al} = 4.45$ in^2

$A_{Ep} = 77$ in^2

$t_{Ep} = 0.030$ in

and for a "hard" epoxy

$G_{Ep} \simeq 0.25 \times 10^{6}$ psi

evaluating equation (9) with these values gives

$$\frac{1}{\Delta T}\left(\frac{\Delta L}{L}\right)_{In} = 17 \times 10^{-6}/^{o}C$$

which is, of course, too large for our purposes. This expansion coefficient corresponds to a thermal stability of 500 MHz/^{o}C for a 1 meter laser cavity operating at 10 microns. To obtain the desired stability we need an effective coefficient of expansion of about 2 - 4 x $10^{-6}/^{o}$C or less, and from equation (9), to obtain this value, the invar rods must be installed and held by an adhesive which exhibits a shear modulus, G , of less than about 200 psi.

This value of shear modulus falls almost into the "rubbery" range and very few materials, which may be useful for our purposes, have published values of G . To find a suitable material we made several test jigs which simply used two metal cylinders, one inside the other, with a 0.030 inch annular gap between them. An adhesive to be tested was used to glue the two pieces together and after the adhesive had set, the unit was tested on a tensiometer. The following results were obtained

Material	G (psi)
Hysol 0266 Epoxy	180
G.E. - RTV 30	120
G.E. - RTV 11	24
Semi-rigid E&C Aluminum Epoxy	> 3 x 10^{4}

The RTV 30 silicone material was used in the fabrication of the laser cavities. As detailed in section 3.1, this material has worked quite well for this application. The aluminum epoxy which exhibits quite high thermal conductivity

was also used on a test cavity and found to be much too rigid. For this case the expansion characteristics of the invar were found to be close to that of the aluminum.

To maintain the cavity at a $\pm$ 0.1°C temperature variation, a proportional type of temperature control system was designed. The design of this controller is detailed in section 2.3.2.

2.2.3 Oscillator Tube Design

During the course of the program, several tube geometries were constructed all of which had approximately the same total length and all had Brewster angle windows, although not all of the windows were the same type material. Some of the tubes were RF excited and others were dc excited, some could be excited with either ac or dc for comparison purposes. Tubes ranging in bore diameters from approximately 50 mm down to sizes of about 6 mm were tested at various times during the program. The results obtained with the RF tubes are discussed in a later section.

The tubes which were used in the final packages were constructed from Pyrex glass. They had an active bore diameter of approximately 7 mm with an overall bore length of approximately 50 cm. It was found that in the testing of various tubes with different bore sizes (see section 3.4) this diameter bore gave consistently high power output in a pure single mode. Larger bore tubes on the order of 8-10 mm quite often ran with second order or third order modes mixed to some degree with the lowest-order mode.

These tubes use a kovar cathode which was constructed in a re-entrant cylindrical configuration. The discharge was run off of the inside diameter of the cathode so that sputtering from one portion of the cathode could be deposited on the other side allowing re-sputtering and liberation of any trapped gases that may have been buried by the sputtering process. In all cases the anode was simply a tungsten pin.

The Brewster angle windows used in the final tubes were constructed from high resistivity (1×10^8 Ω-cm) GaAs. The absorption coefficient of this material was measured to be approximately the same as good quality optical grade germanium (.01 per cm) but does not suffer the thermal runaway problem to the extent that germanium does. The tube also contained a reservoir volume of approximately 1/3 liter. Since the laser tube was water-cooled the ballast resistors used with the tube were also placed in a water-cooled jacket. This allowed a much smaller size resistor string to achieve the same power dissipation capability.

For the above size bore and length of the laser tube the optimum current and voltage for the laser was approximately 15 kv at 12 milliamperes. Powers ranging up to 8 watts were observed from this laser when a 14% transmission output mirror was used. The above powers were obtained with a gas mixture of 1 torr Xe, 6 torr CO_2 and about 14 torr He. The Xenon was used in an attempt to achieve lower operating and breakdown voltages and longer operation life[4].

2.2.4 Amplifier Design

Several amplifier tubes were constructed during the program. The first of which being RF excited. This tube was used in early tests on measurements of gain versus pressure and is described in detail in section 3.3. In all cases the amplifiers used a bore diameter of approximately 19 mm. The active length was approximately 180 cm and the amplifiers utilized an internal mirror at one end of the tube for beam-folding purposes.

In the final package two amplifier tubes were used. The tubes were placed optically in series, but mechanically in parallel. Figure 4 is an assembly drawing of one of the amplifier tubes used on the program. The main support structure for the amplifier tube is a two-inch diameter Pyrex tube which extends about 1 1/2 meters between the two amplifier tubes. This large diameter tube also served as a gas ballast-volume for the amplifiers.

The input end of the amplifiers were cut at Brewster's angle and potassium-chloride windows were used. Two amplifier systems of this basic design were constructed. The first as shown in Figure 4 utilized mirrors internal to the vacuum system which were adjustable through the bellows assembly. A later tube, shipped with the final unit, did not use the bellows assembly but had fixed position mirrors epoxied to the end of the amplifier glass envelope. This feature was found desirable from a mechanical rigidity viewpoint as well as allowing a much simpler procedure for mirror alignment, since in the latter case the front surface of the fixed mirrors could be observed through the glass walls of the amplifier, and a helium-neon laser beam could be traced through the amplifier.

In actual operation the oscillator beam was passed through the bottom of the lower amplifier tube and after reflection from the fixed internal mirror the beam was then brought out of the bottom amplifier tube on the high side of the Brewster-angle window. The beam sizes were sufficiently small so that the input and output beams could be separated. The beam was then folded by external optics up to the top of the amplifier tube. The beam was double-passed through the top amplifier tube before passing out of the laser structure. This folded optical path is depicted in Figure 5 which is an overall assembly drawing of the oscillator-amplifier system.

To control the beam size as the oscillator beam passed through the amplifier tube and to insure that the beams could be separated completely at the folding optics near the front of the amplifier, the internal mirrors in the amplifier were chosen to have front surface curvature. The lower mirror had a radius of curvature of 3.12 meters while the upper mirror had a radius of curvature of 4.67 meters. These mirrors provide a well-collimated output of about 8 mm in diameter. The divergence was estimated at about 3 milliradians.

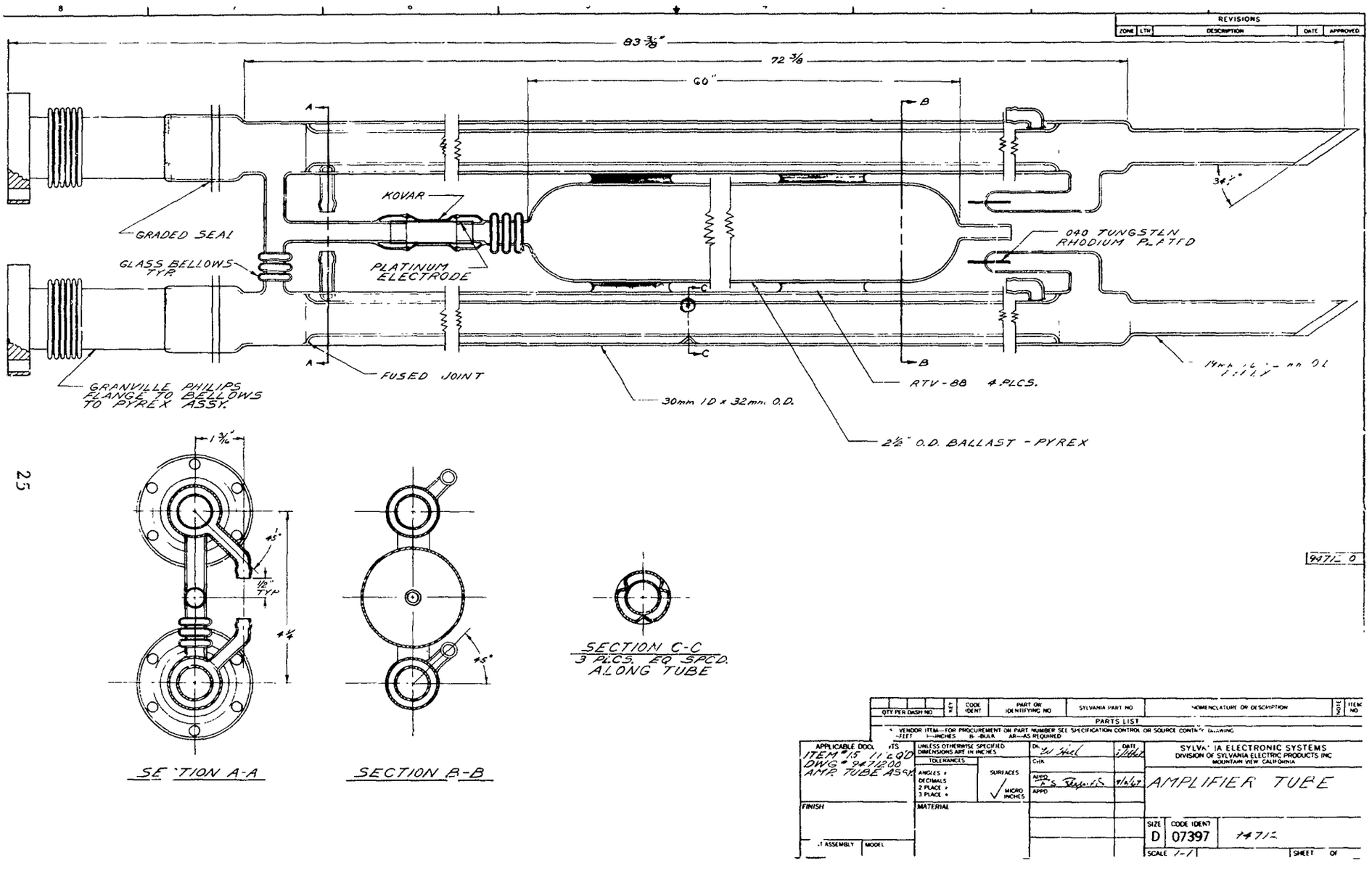

QTY PER DASH NO	KEY	CODE IDENT	PART OR IDENTIFYING NO	SYLVANIA PART NO	NOMENCLATURE OR DESCRIPTION	ITEM NO
PARTS LIST						

VENDOR ITEM—FOR PROCUREMENT OR PART NUMBER SEE SPECIFICATION CONTROL OR SOURCE CONTROL DRAWING
FIET I—INCHES B—BULK AR—AS REQUIRED

APPLICABLE DOCUMENTS
ITEM #15 11 c 9D
DWG # 9471200
AMP. TUBE ASSY

UNLESS OTHERWISE SPECIFIED DIMENSIONS ARE IN INCHES
TOLERANCES
ANGLES °
DECIMALS
2 PLACE ±
3 PLACE ±
SURFACES
MICRO INCHES

DR. W. Hall 9/6/67
CHK
ADDO. A.S. Stephens 9/6/67
APPD

SYLVANIA ELECTRONIC SYSTEMS
DIVISION OF SYLVANIA ELECTRIC PRODUCTS INC
MOUNTAIN VIEW CALIFORNIA

AMPLIFIER TUBE

FINISH
MATERIAL
NEXT ASSEMBLY | MODEL

SIZE D | CODE IDENT 07397 | 9471-C
SCALE 1-1 | SHEET OF

Figure 4. Laser Amplifier Tube.

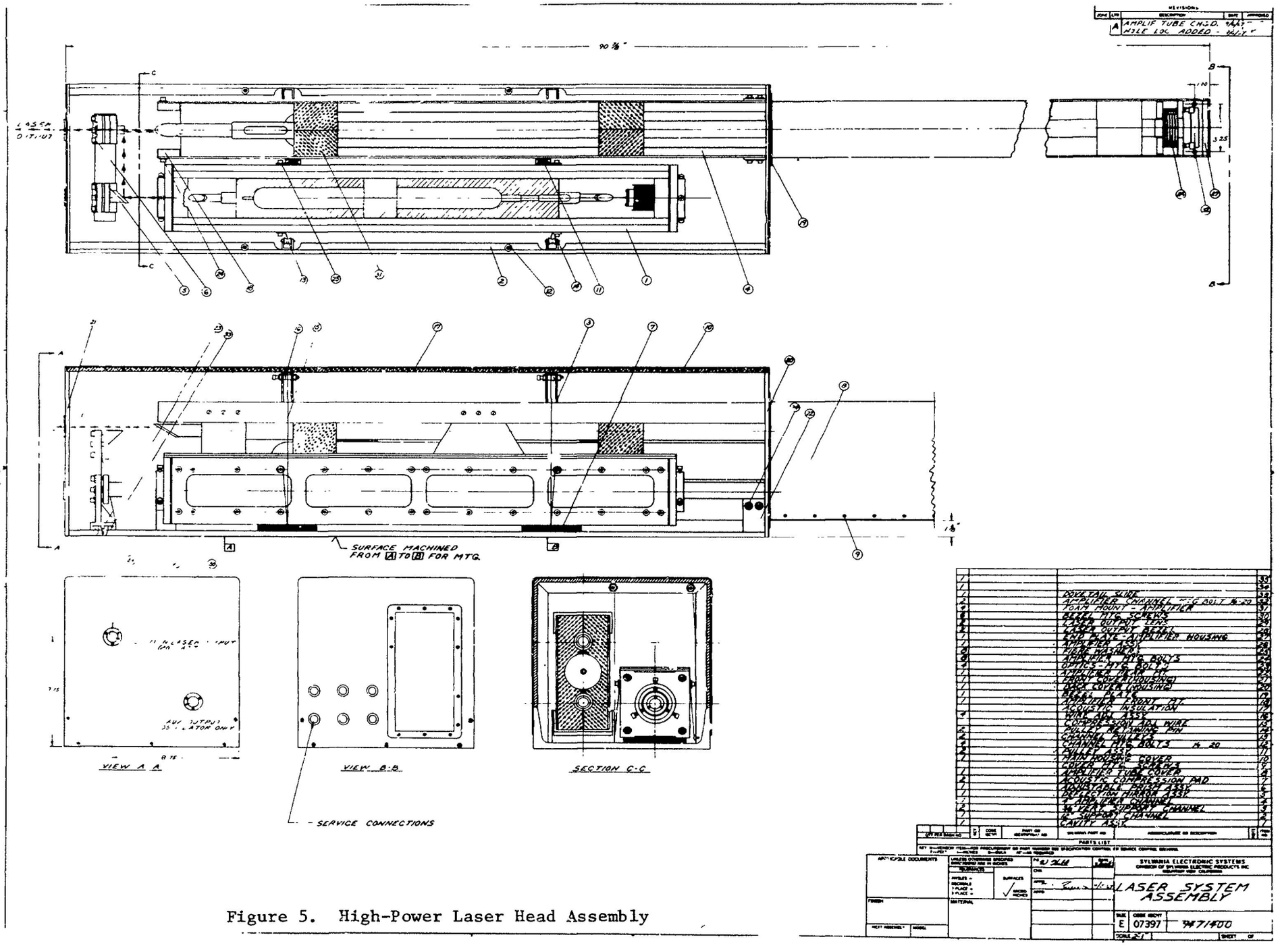

Figure 5. High-Power Laser Head Assembly

2.2.5 Heat Exchanger

The laser system also contains a recirculating laser cooling system depicted schematically in Figure 6 which is capable of cooling the laser tube to about 15°C during operation. To maintain a relatively constant thermal load at the laser, the cooling unit contains a coarse temperature control system of the thermostatic type.

A small refrigeration (Freon) unit capable of handling about 800 watts was used on the primary side, while water was circulated to the laser on the secondary side. To reduce the effects of vibration from the water circulating pump, an accumulator was installed in the line at the outlet of the cooling unit proper. Since the laser only requires approximately 1/4 gpm to maintain a satisfactorily low temperature, a bypass line was installed around the heat exchanger-pump combination so that high velocities through the heat exchanger could be maintained. The higher flow rates through the exchanger allows for more efficient primary cooling.

The flow system has been interlocked for insufficient flow and excess coolant temperature to protect the laser tube and ballast resistors (which are water cooled).

The freon system utilizes a continuously operating compressor. Temperature control of the water is controlled by the use of a bypass solenoid valve which diverts the freon liquid to an auxiliary evaporator for a fractional period of time. The proportion of time that the liquid is diverted is controlled by the adjustable temperature control unit. The continuously operating feature of the compressor systems reduces current surges on the line which could be reflected in the laser output through the dc power supplies.

2.3 Electrical Design

Figure 7 contains the electrical schematic of the 20+ watt laser head. The amplifier system consists of two parallel tubes connected

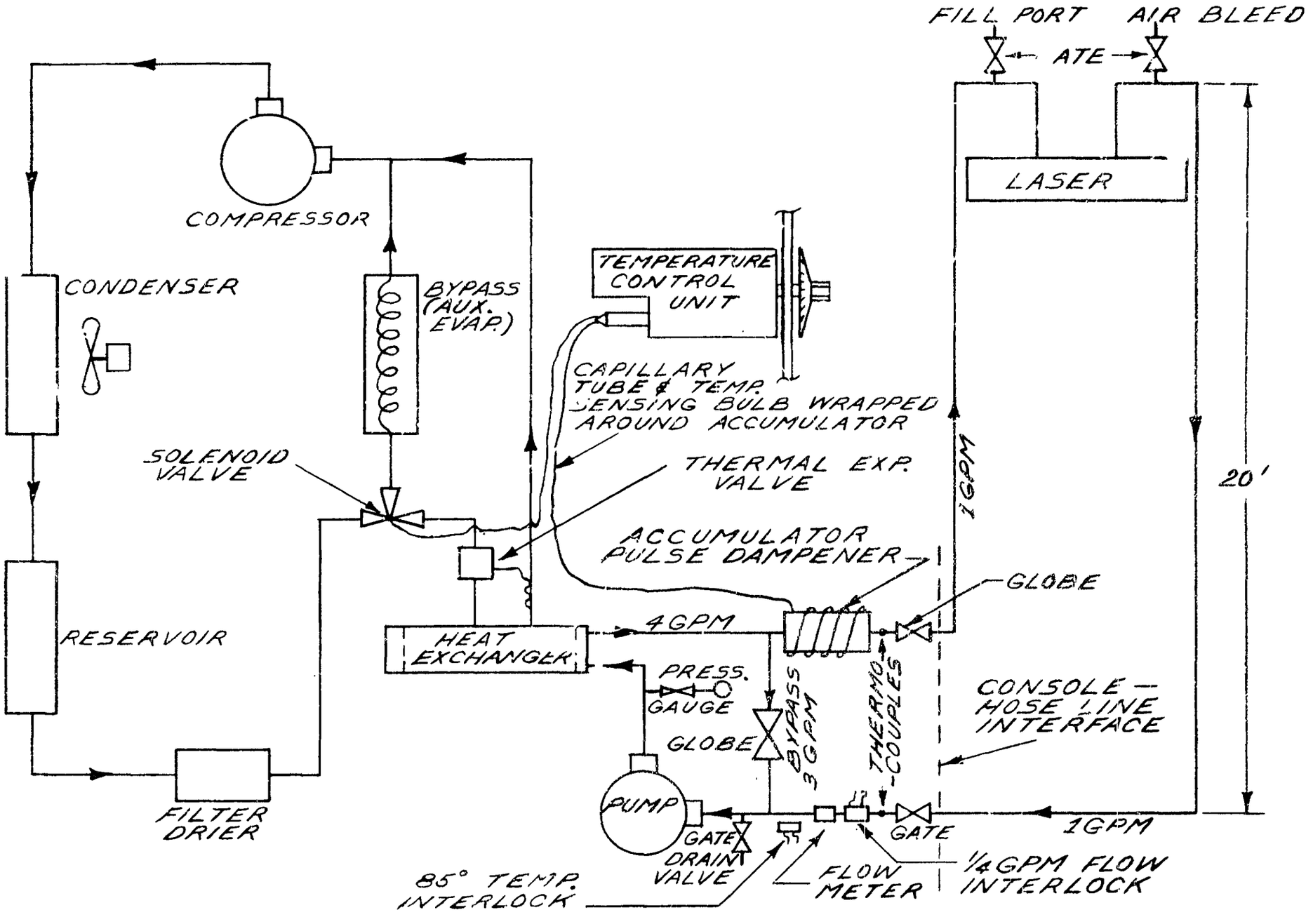

Figure 6. Twenty-Watt Laser Cooling System.

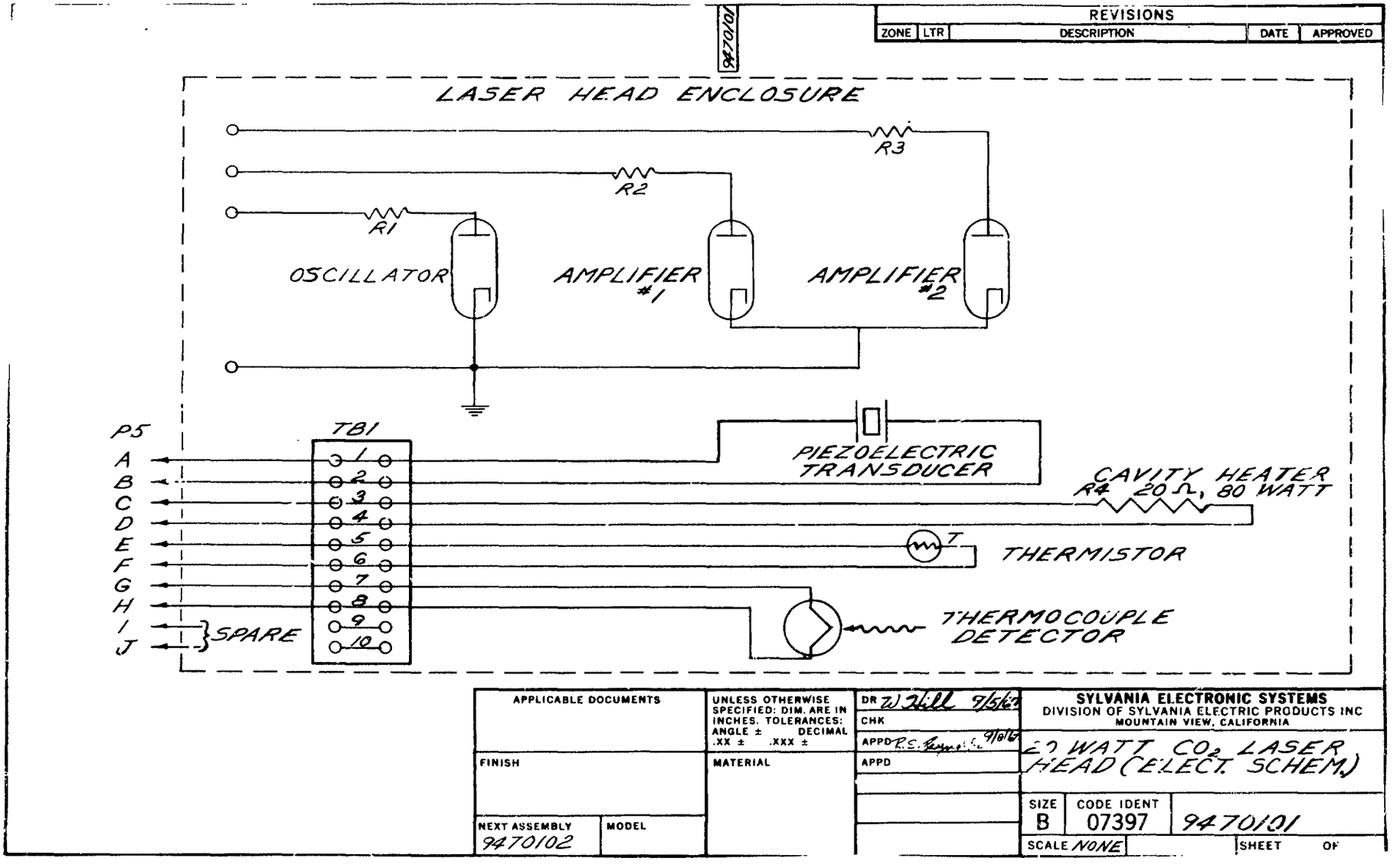

Figure 7. Electrical Schematic of High-Power Laser Head

to a common cathode and ballast tank. Each amplifier tube is driven by its own power supply so that each tube can be operated separately. The excitation level of each tube can be controlled at the power supply to provide virtually any level of amplification up to the maximum value. The ballast resistors R1, 2, 3 were all set at 400kΩ. It was found that substantially lower figures created instabilities in starting and during operation.

The laser power console is shown schematically in Figure 8. The console houses the individual power supplies for the oscillator tube, each amplifier, and the piezoelectric transducer, as well as the temperature control electronics and heat exchanger. These items are discussed in more detail below.

2.3.1 High Voltage Supplies

The dc power supply for the laser oscillator is a Sorenson Model 1020-30 which is capable of providing 20 kv at 30 ma. With the final oscillator design, the laser tube only requires about 15 kv at about 10 ma, so the power supply only operates at about 1/4 of its capability. The amplifier tubes use Sorenson Model 1030-20 supplies which are capable of providing 30 kv at 20 ma. Each amplifier tube, however, operates at a supply voltage of 20 kv and a current of about 15 ma. The above figures include the drop in the ballast resistors.

The line and load regulation for th e units are provided by a regulating transformer which electrically precedes the console. The power supplies are fully metered so that the current and voltage can be monitored, if desired. Over voltage and current interlocks are included as well as coolant flow and temperature interlocks. Each of the high voltage power supplies are filtered to provide a $\pm$ .01% ripple figure. As will be described later in the section on frequency stability measurements, further reduction in the power supply ripple figure would probably be necessary if greater stabilities are desired.

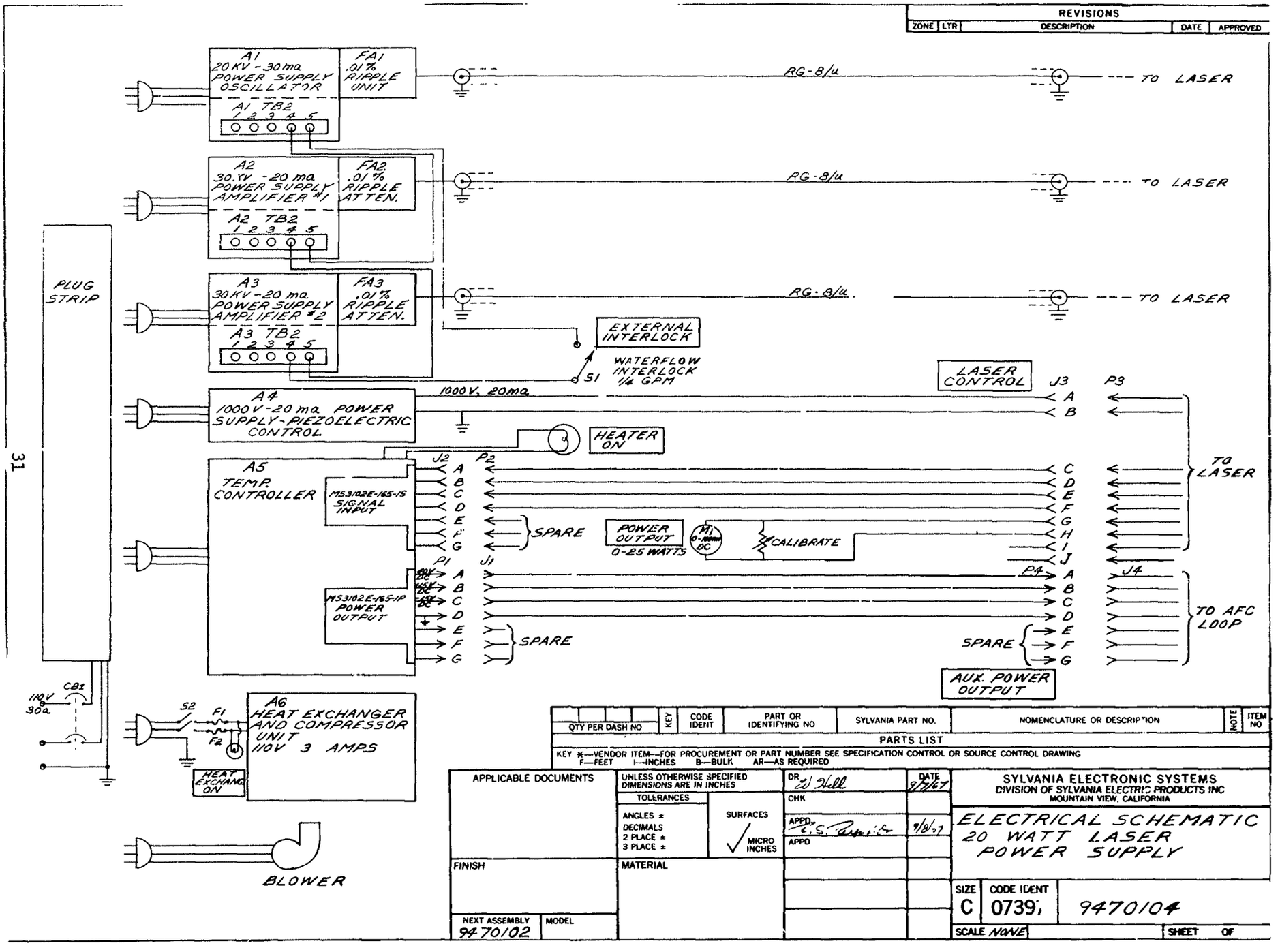

Figure 8. Electrical Schematic of High-Power Laser Power Supply

2.3.2 Temperature Controller

The temperature controller, designate A3 in Figure 8 utilizes a bridge network in which a high-sensitivity thermistor, mounted on the laser cavity, serves to provide a continuous error signal to a differential amplifier. The output of the amplifier controls the bias setting on a set of current controlling transistors which regulate the amount of power delivered to the cavity heater. The cavity heater is a low density 24" long resistive strip capable of dissipating 80 watts. The heater is fastened to the bottom of the aluminum cavity structure.

The circuit shown in Figure 9 is designed to maintain the laser cavity to within $\pm$ 0.1°C at a temperature of about 40°C. A bias adjust setting of 2.8 volts at TP2 (at the input of A2) allows approximately one amp nominal current to flow through the heater. The heater thus nominally dissipates 20 watts of power. This 2.8 volt figure is modified by the output of amplifier A1. It adds or substracts from this value depending upon whether or not the voltage across the thermistor is larger or smaller than the bridge reference voltage. The bridge reference voltage is set by the 1200 Ω resistor R6.

Figure 10 shows the temperature-resistance characteristics of the thermistor used. This particular unit was chosen because of its high dR/dT near the desired operating temperature of 40°C. The thermistor is mounted on a miniature connector attached directly to the aluminum laser cavity.

About the 40°C temperature point, for every .1°C change in thermistor temperature, the bridge unbalance corresponds to about 2 mv. This unbalance is multiplied by the product of the gains of A1 and A2 (10 each) resulting in a 200 mv output from A2. Thus, about the 2.8 volt bias point, the change in heater dissipation is about 8 watts/.1°C change in thermistor temperature.

Figure 11 is a photograph of the temperature control unit. The control electronics are mounted under the chassis while two dc power supplies are

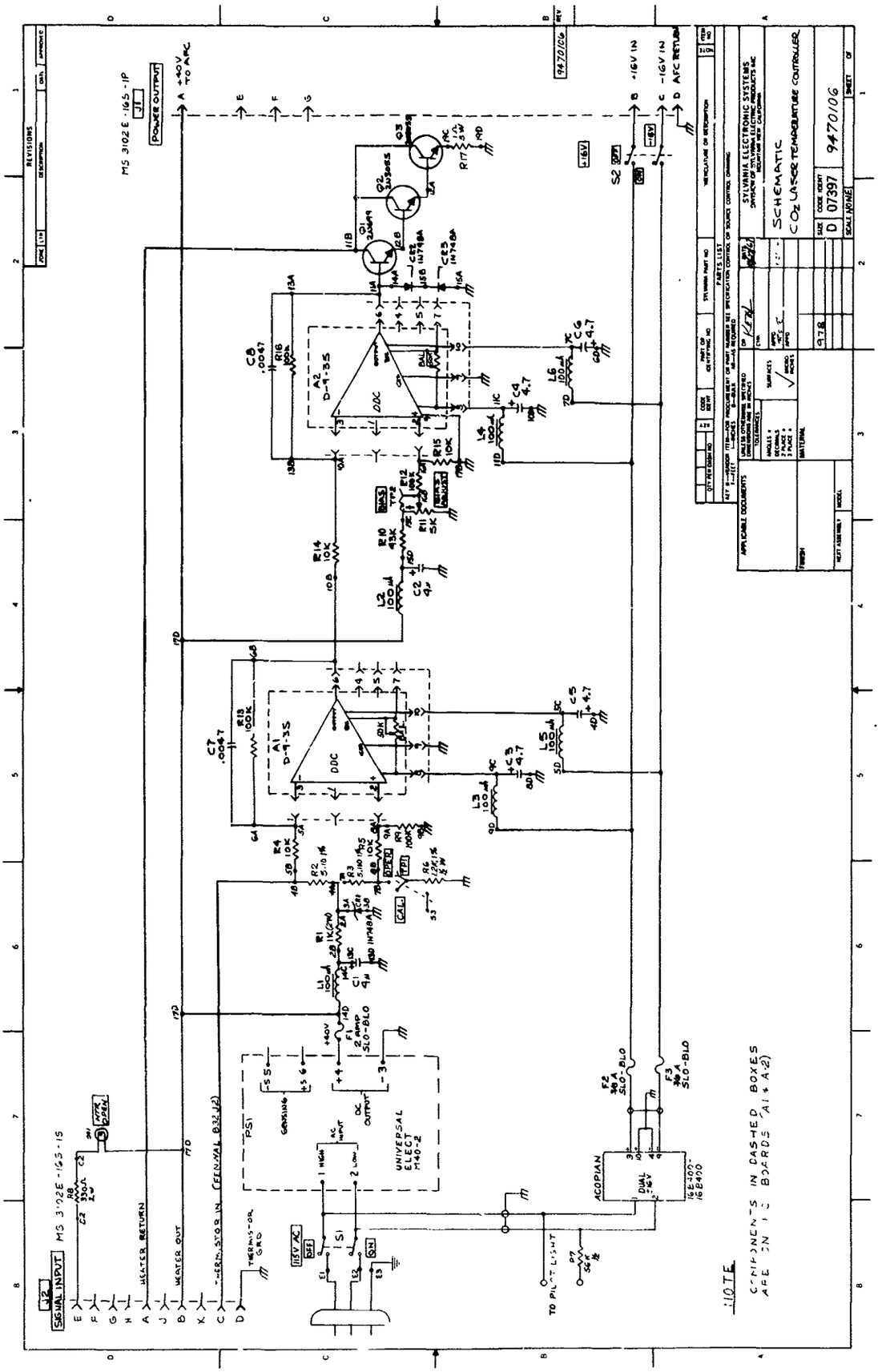

Figure 9. Schematic of CO_2 Laser Temperature Controller

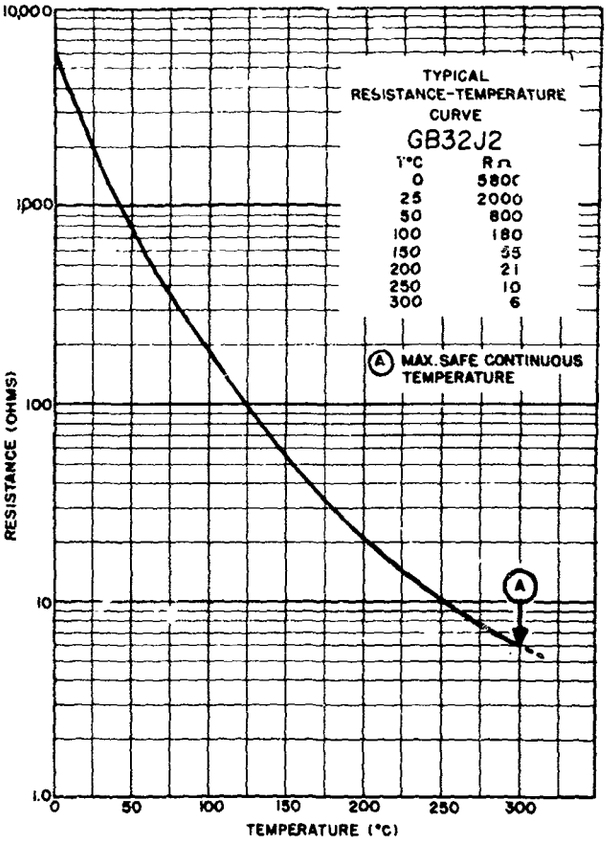

Figure 10. Thermal Characteristic of the Thermistor Used in the Laser Temperature Control Electronics

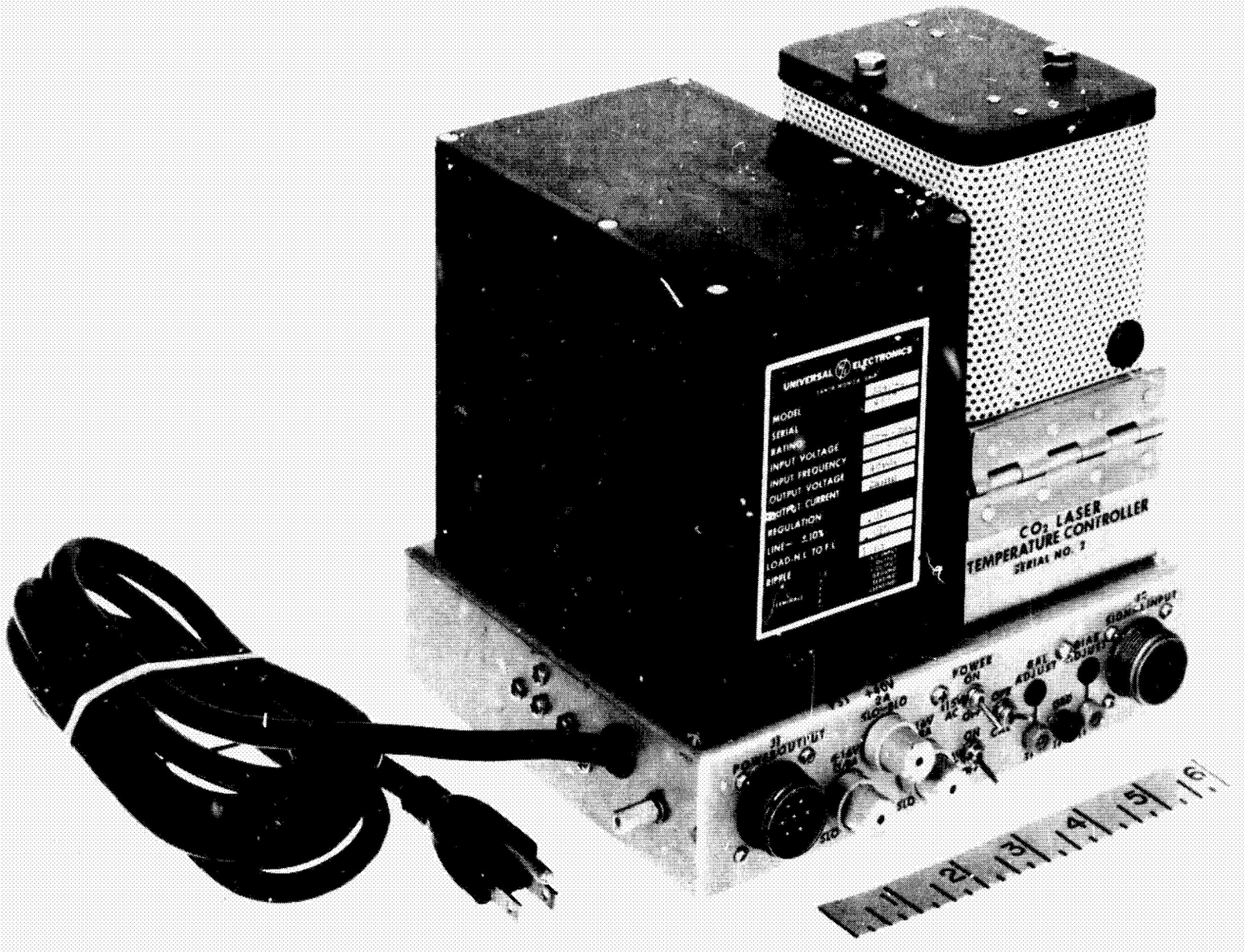

Figure 11. CO_2 Laser Temperature Controller

mounted on top. The larger power supply provide 80 watts of dc power to the cavity heater. The smaller supply provides bias voltages to the differential amplifiers used in the control loop. DC power is supplied to the heater rather than ac power in order to eliminate the possibility of magneto-strictive length changes in the cavity caused by varying fields near the invar rods.

In normal operation the temperature controller is left on continuously in order to minimize warm-up time whenever the laser is turned on. If the heater is left off, the warm-up time for the unit is about two hours. This can be compared with a warm-up time of less than 1/2 hour if the heater is allowed to remain operational.

2.3.3 Frequency Adjust Electronics

The laser frequency control power supply, designated A4 in Figure 8 is a 1000V, 20 ma dc power supply manufactured by KEPCO. The supply (model 1000 ABC M) is capable of operating either as a simple dc power supply or with minor adjustments as a high voltage dc amplifier.

This supply allows controlled manual or automatic physical movement of the non-transmitting laser mirror which in turn allows the operating frequency of the laser to be controlled and adjusted. The power supply has a coarse and a fine control of the output-voltage, allowing the laser frequency to be accurately adjusted to within about 50 kHz manually.

The main electrical control element consists of a special piezoelectric transducer with 40 individual plates mechanically connected in series and electrically connected in parallel. Each plate has a thickness of .030 inches and a diameter of 1 3/4 inches. The length-to-width ratio of the stack has been chosen for good mechanical stability. The device is capable of about 15 microns of movement for an applied voltage of 800 volts. Because of its large capacitance, its basic corner frequency is about 200 Hz; however, a

single piezoelectric plate, electrically isolated from the rest of the transducer structure and mounted on the mirror side of the transducer, extends the usable frequency response to over 5 kHz. If desired, the unit can be used in a feedback control system.

The sensitivity of the power supply transducer system for this laser is about 3/4 MHz/volt. That is, the laser output frequency is changed by 3/4 MHz for every volt change in supply voltage. Since the Doppler linewidth of the CO_2 laser transition is about 50 MHz, a $\pm$ volt change in the transducer supply voltage is all that is necessary to scan the gain curve of a particular wavelength.

Although the laser generally operates in only a single wavelength, it is possible to select the output wavelength from the laser by adjusting the transducer voltage in 50-100 volt increments.

2.4 Completed System

The completed laser is shown in Figure 12. The oscillator, folding optics and part of the amplifier are located in a 12" x 12" x 48" enclosure with the amplifier extending beyond the enclosure in a 6" x 8" x 48" long lightweight container. An adjustable output lens (KCl) has also been included so that the laser beam can be focused through a 3 mm x 3 mm modulator (used at the final installation) located about 26 inches from the front of the laser.

The individual power supplies for the oscillator and two amplifier tubes occupy the top portion of the power supply console, the laser frequency control electronics, temperature controller, cabinet fan and heat exchanger fill the remainder of the console. Sufficient length of hoses and cables have been provided so that the power supply console can be operated at a distance of up to 45 feet from the laser head.

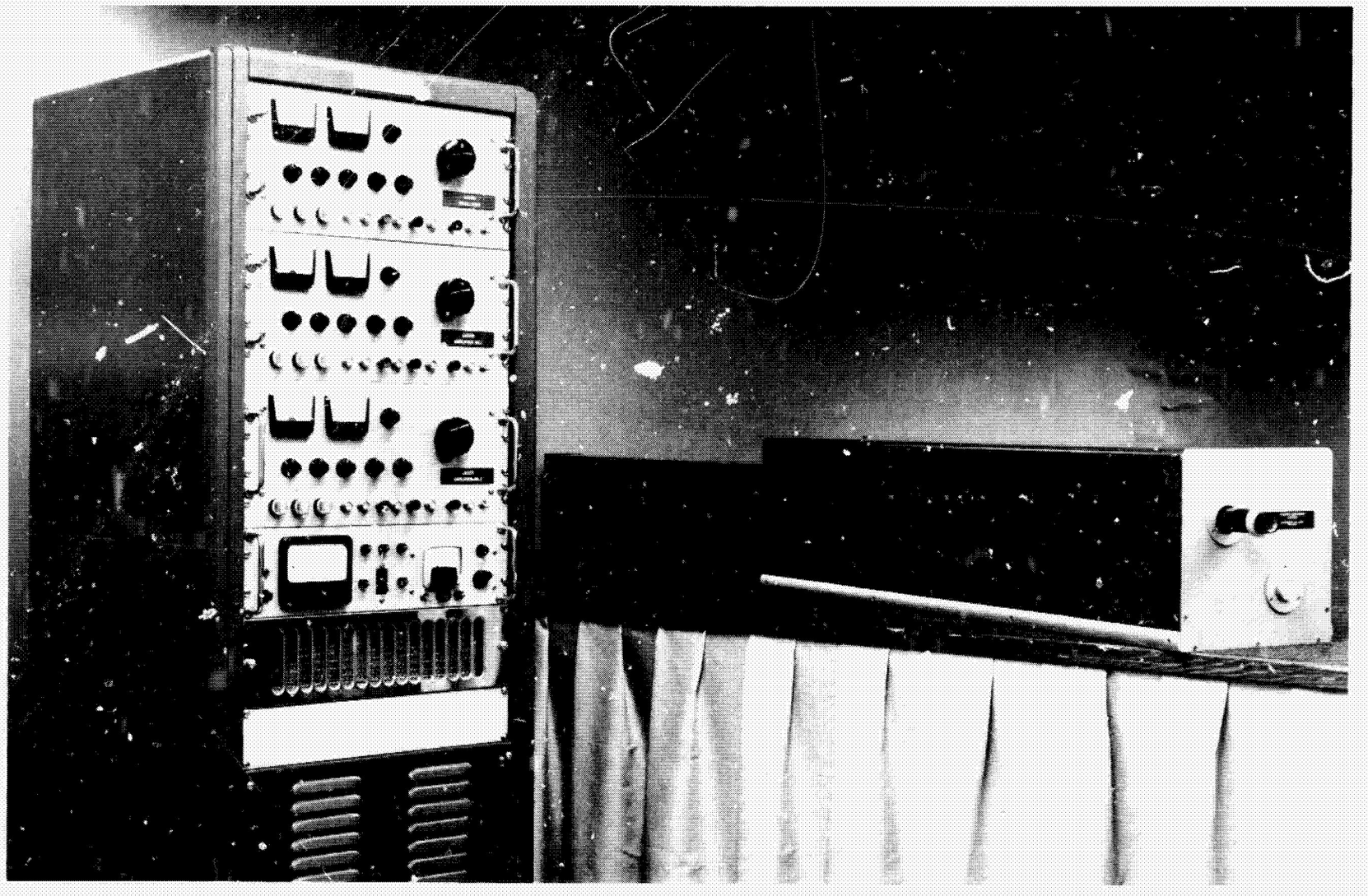

Figure 12. Completed High Power Laser

2.5 Auxiliary Oscillator

The auxiliary oscillator constructed on this program for checking the stability of the high power laser utilized a laser cavity and laser tube identical to that used in the high power laser. Figure 13 is an electrical schematic of the laser and its power supply. In this case the laser uses water cooling from the city water supply, however, the high voltage power supply, piezoelectric transducer power supply and the temperature control electronics are identical to those described earlier. Most of the mounting hardware and the vibration inhibiting enclosure is identical to that used in the high power laser so that the auxiliary oscillator can be used as a backup for the high power laser, if necessary.

The auxiliary laser utilizes a 6% transmitting flat output mirror (multilayer dielectrically coated on an IRTRAN 2 substrate) with a 3.12 meter gold coated quartz mirror mounted on the piezoelectric transducer. The laser emits about 3 watts single frequency in the TEM_{ooq} mode. Although a higher transparency mirror allows this laser to emit higher powers, it was found that a greater number of wavelengths could be selected with the 6% transmission mirror. This feature can be important since during heterodyne tests the auxiliary oscillator must be tuned to the wavelength for which the high power laser has the greatest output (generally 10.59 microns).

Figure 14 is a photograph of the 3 watt auxiliary laser. The enclosure for the laser is tightly sealed with a BaF_2 output window. The laser head measures about 12" x 12" x 48" and weighs about 100 lbs.

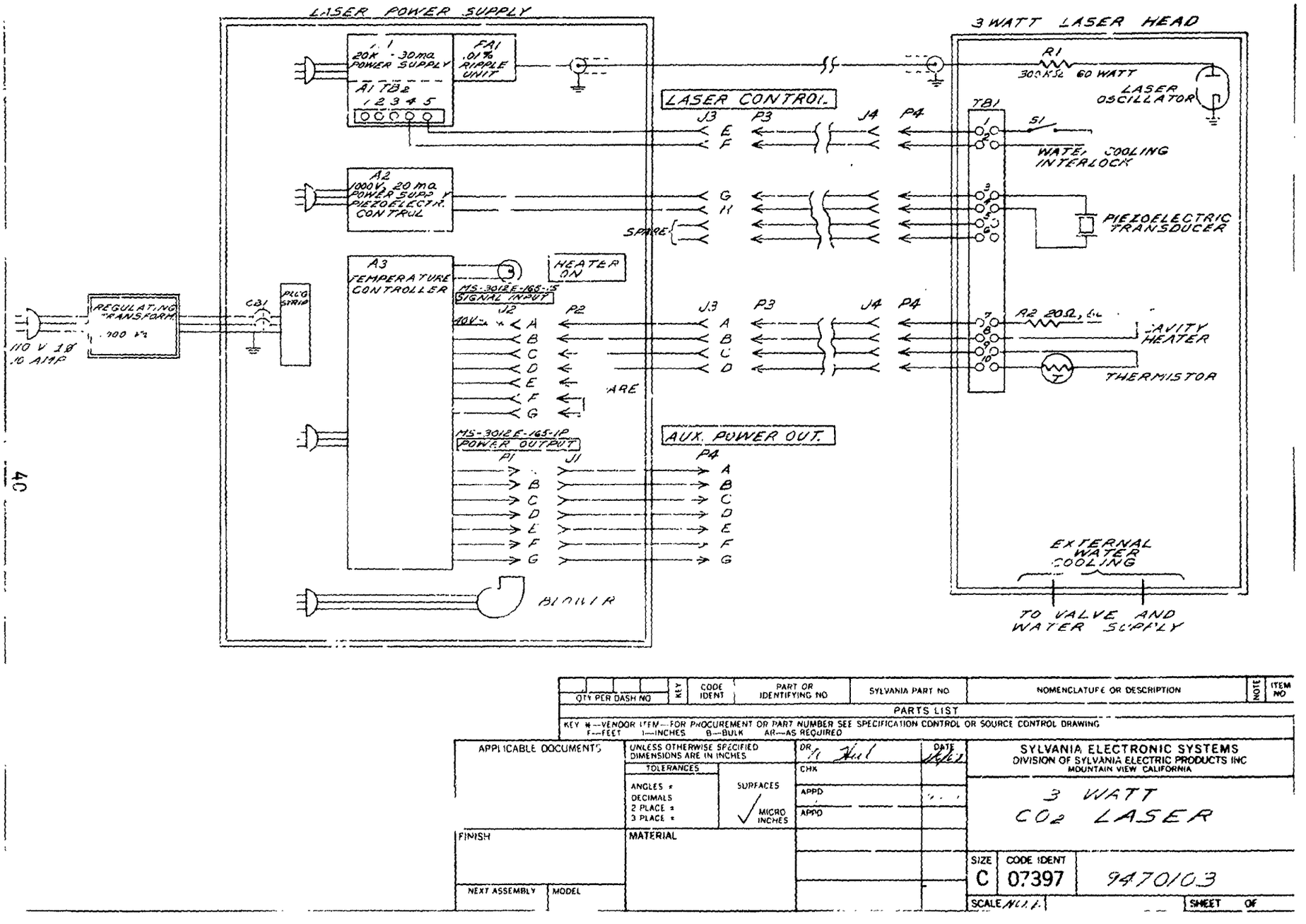

QTY PER DASH NO	KEY	CODE IDENT	PART OR IDENTIFYING NO	SYLVANIA PART NO	NOMENCLATURE OR DESCRIPTION	NOTE	ITEM NO

PARTS LIST

KEY W—VENDOR ITEM—FOR PROCUREMENT OR PART NUMBER SEE SPECIFICATION CONTROL OR SOURCE CONTROL DRAWING
F—FEET I—INCHES B—BULK AR—AS REQUIRED

APPLICABLE DOCUMENTS

UNLESS OTHERWISE SPECIFIED DIMENSIONS ARE IN INCHES
TOLERANCES
ANGLES ±
DECIMALS
2 PLACE ±
3 PLACE ±
SURFACES
√ MICRO INCHES

FINISH

MATERIAL

NEXT ASSEMBLY | MODEL

DR R. Hull DATE 10/6/72
CHK
APPD
APPD

SYLVANIA ELECTRONIC SYSTEMS
DIVISION OF SYLVANIA ELECTRIC PRODUCTS INC
MOUNTAIN VIEW CALIFORNIA

3 WATT
CO_2 LASER

SIZE C | CODE IDENT 07397 | 9470103

SCALE N.C.I.A. SHEET OF

Figure 13. Electrical Schematic of Three-Watt CO_2 Laser

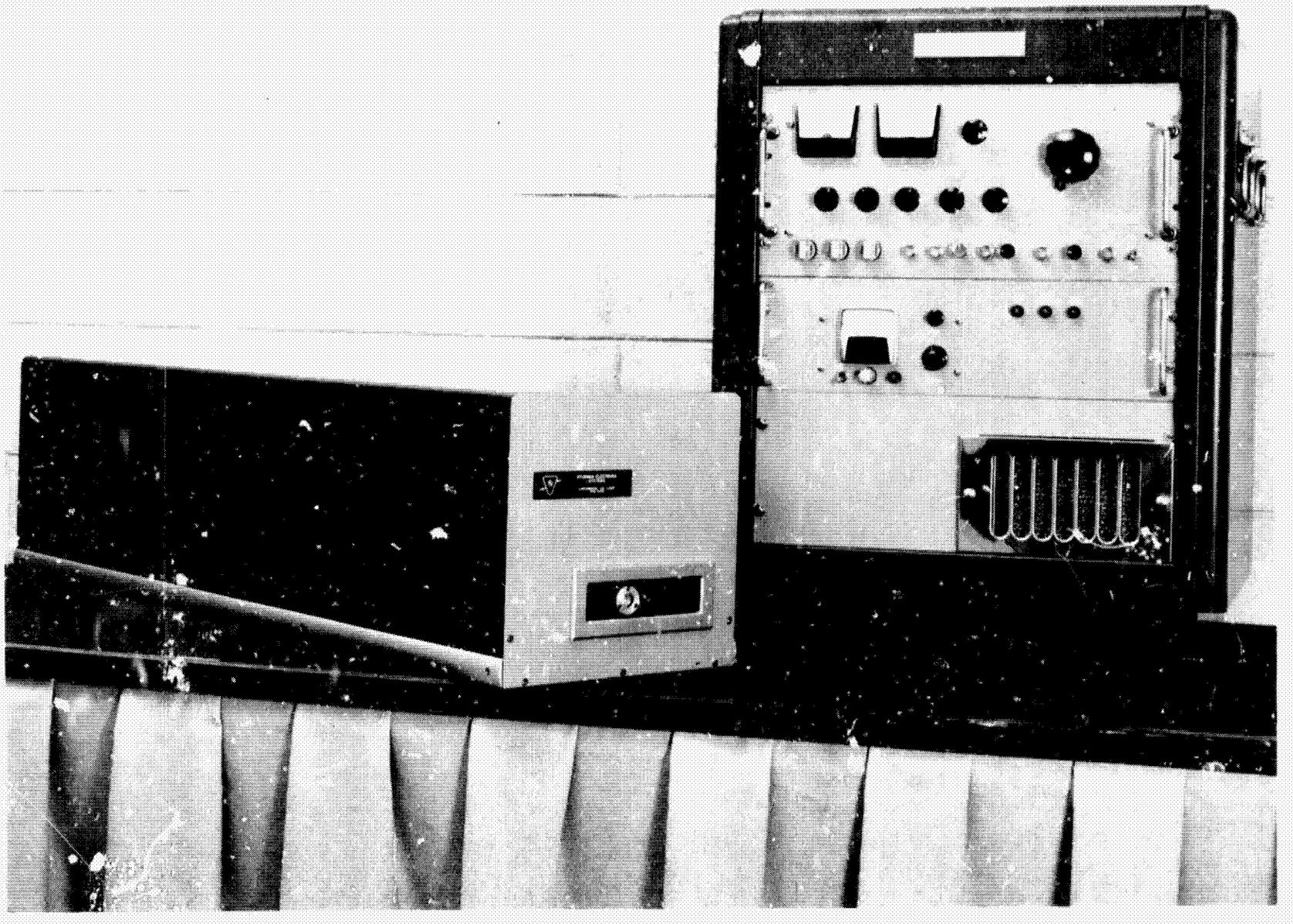

Figure 14. Three-Watt Auxiliary Laser

3.0 EXPERIMENTAL RESULTS

During the course of the program several tests and experiments were performed in order to gather data necessary for the design and operation of the laser system, and to measure the operating characteristics of the lasers. The tests included: laser cavity thermal tests, RF excitation studies, effects of bore size on single mode output power, amplifier gain studies, vibration tests and frequency stability measurements. The results of these tests are described below.

3.1 Laser Thermal Tests

As was discussed in section 2.2.2, the thermal stability of the combination invar-aluminum cavity is determined by the invar only if the aluminum does not mechanically drag the invar with it as it expands or contracts. To determine the effect of several types of adhesive materials, two test cavities were fabricated with laser tubes installed. In one cavity RTV 30 was used as an adhesive between the invar rods and the aluminum structure, while in the second cavity a "semi-rigid" aluminum epoxy was used. The aluminum epoxy was chosen because of its relatively high thermal conductivity, an advantage in maintaining a good thermal environment for the invar, and the RTV 30 was used because of its low shear modulus of elasticity.

The lasers were operated with the temperature control system inoperative, and the outputs of the lasers were monitored through a monochromator. After the cavities had come to thermal equilibrium, the cavity with the RTV 30 would remain on a single transition for periods up to several hours while the output of the cavity with the aluminum epoxy could only be kept on a particular wavelength for a period of a few minutes before it would drift to a new wavelength.

The cavities were then heated by the thermal control system, and the temperature rise of the cavities observed as a function of time. Simultaneously, a calibrated piezoelectric stack, onto which one of the laser mirrors was attached, and a voltage variable d.c. voltage source, were used to maintain the same output wavelength from each of the lasers as the temperature was increased. The absolute expansion rates were then obtained for the laser cavities.

The measured effective coefficients of expansion of the two cavities are given below:

Adhesive Material	α (Cavity)
RTV 30	$2 \times 10^{-6}/^{o}C$
"Semi-rigid" aluminum epoxy	$22 \times 10^{-6}/^{o}C$

These numbers fall very close to those predicted by the theory presented in section 2.2.2. The aluminum epoxy, which creates an expansion characteristic very similar to just the aluminum structure, would not be adequate for use in this application. The RTV 30, however, has proved to be quite satisfactory.

In later tests, after the thermal control unit was controlling to $\pm 0.1^{o}C$, the laser with the RTV 30 bonding, would operate for an indefinite period of time on a single transition. The laser would also operate on the same wavelength on a day-to-day basis, although the initial operating conditions had to be accurately repeated. That is, the laser tube current, water flow rate, and piezoelectric transducer voltage had to be set close to the previous day's values. Approximately 1/2 hour warm-up time was required before stable operation was obtained.

3.2 Cavity Vibration Tests

As described in section 2.2.1, the laser cavity was designed to be a very rigid assembly within the limits of the thermal and weight requirements. The main purpose for the rigid construction is to achieve as high a lowest order longitudinal resonance as possible for the basic length of the laser. For the 92 cm long cavity, it was expected that the lowest order longitudinal resonance should occur at a frequency of about 2700 cps.

To check the resonance characteristics of the laser cavity and to determine the lowest fundamental resonances, the laser cavity was tested utilizing two

piezoelectric transducers. An excitation transducer fabricated from a stack of piezoelectric plates was located on the mirror mount at one end of the cavity, while a similar transducer serving as a pick-up head was located at the other mirror mount. The vibration intensity at the pick-up transducer was measured as a function of excitation frequency using an oscilloscope as the read-out instrument.

Figure 15 shows the results of the measurement. The lowest order longitudinal resonance occurs at 2530 cps, near the expected value of about 2700 cps. Several weaker resonances at lower frequencies were observed and are attributed to transverse resonances. No resonances could be detected below about 1100 cps.

The same test was run on a similar channel shaped cavity of 50 cm length which happened to be available. The main difference between the shorter cavity and the 92 cm invar-aluminum cavity was the type of mirror mounts used. The short cavity used thick steel plates onto which the mirror was rigidly clamped. However, to obtain mirror adjustment capability, the plates were clamped to the ends of the channel with three sets of push-pull screws. This arrangement allows only the small contact area determined by the screws in joining the end plates to the cavity and is quite susceptible to low frequency transverse vibrations.

Several large resonances were observed as low as 400 cps even though the mirror mounts were tightly clamped. The resonant frequencies could be tuned somewhat by applying an external force to the mirror mount. By removing the adjustment screws and bolting the plates rigidly to the end of the cavity, the low frequency resonances disappeared. These tests dramatically indicated the necessity for large area, tightly clamped joints.

3.3 RF Excitation Studies

Various tubes were constructed which could be excited with either d.c. or RF power. In all cases the tubes utilized Brewster angle windows made from potassium chloride. KCl was used for its superior hygroscopic properties over the less costly NaCl. The bore sizes for the various tubes ranged from 50 mm

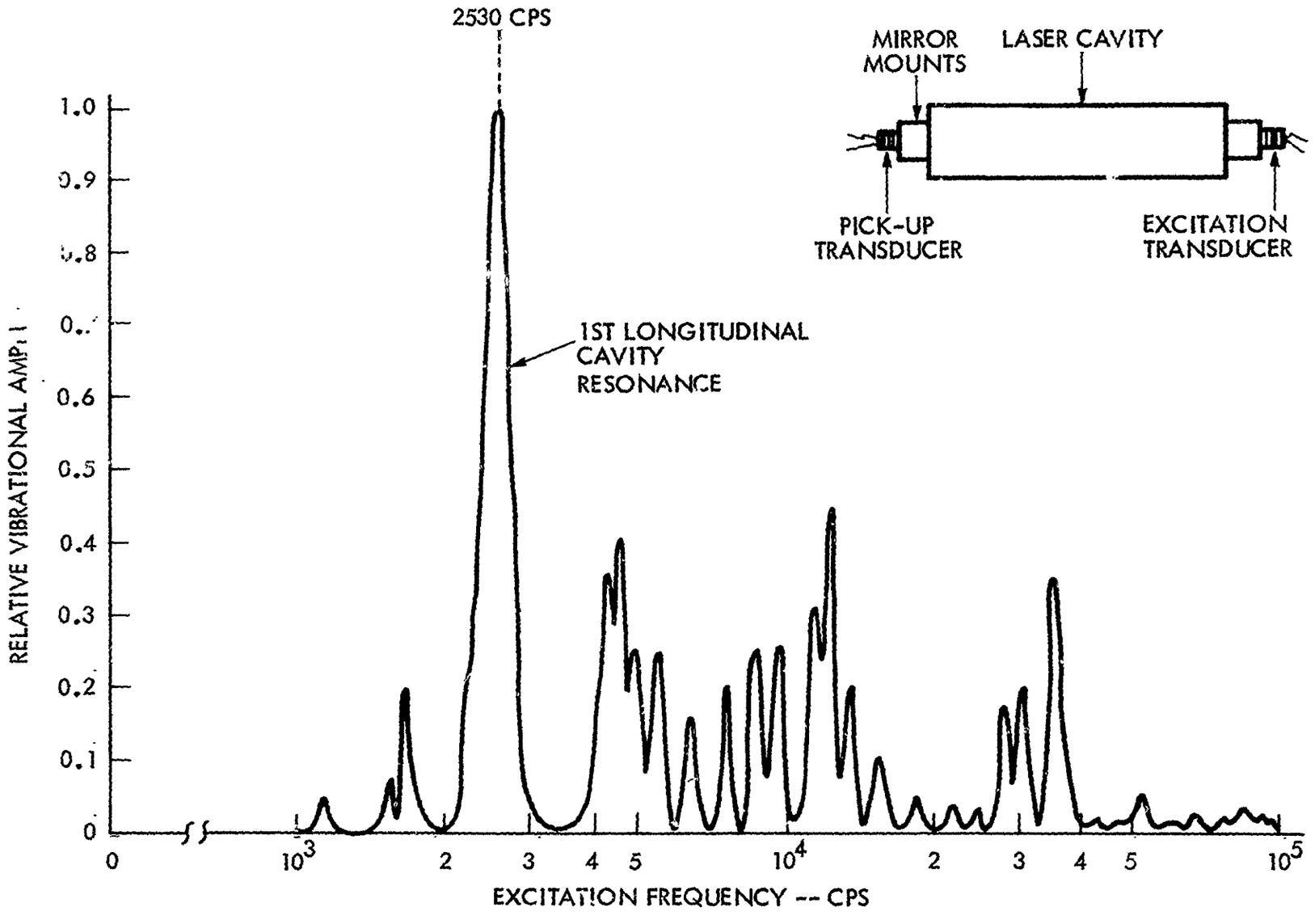

Figure 15. Resonances of the CO_2 Laser Cavity Structure.

to 6 mm, and various techniques were attempted to determine the optimum method for introducing the RF power into the laser.

Compared to the He-Ne laser, the CO_2 laser requires much higher RF voltages to break the gas mixture down. For this reason our attempts using a series of ring electrodes down the length of the discharge tube was not entirely successful. The most satisfactory geometry was found to be simple strip electrodes placed on either side of the laser tube. Although a dual strip helix wrapped around the tube with a pitch approximately equal to the strip spacing was found to work quite well, the discharge distribution was not as uniform inside the tube as the case of the parallel electrodes.

Because of the high voltage requirements for gas breakdown, much care must be taken in the design of the RF matching network if efficient power transfer is to be obtained. Figure 16 shows the network we used for both the laser tubes and the amplifier tubes. One major advantage with this circuit is that the unbalanced 50 Ω output from the RF transmitter is converted to a balanced line at the laser. With this technique, little radiation to surrounding grounded structures is realized. This feature then allows matched operation of the laser even when its surrounding ground plane geometry is changed. The laser could be moved from the processing station and installed in the metal laser cavity without any adjustment in the matching network. Also the metal covers to the laser structure could be removed and replaced without changing the operating characteristics of the laser. The matching network used a two-turn primary closely coupled to a 12-turn secondary of about 1" in diameter. The variable capacitors were chosen to resonate the primary and secondary at the operating frequency which was 27 MHz for the laser oscillators.

Without cooling the walls of the discharge tube, the laser output power would dwindle to a very low value in only a short time after turn-on. In most cases it was found advantageous to use a silicone cooling fluid such as DC 200 since with its low dielectric constant, the RF could be passed directly through it to the discharge region. Unfortunately, the dielectric constant of water is so great that the RF field essentially becomes trapped in the water and never penetrates the discharge region.

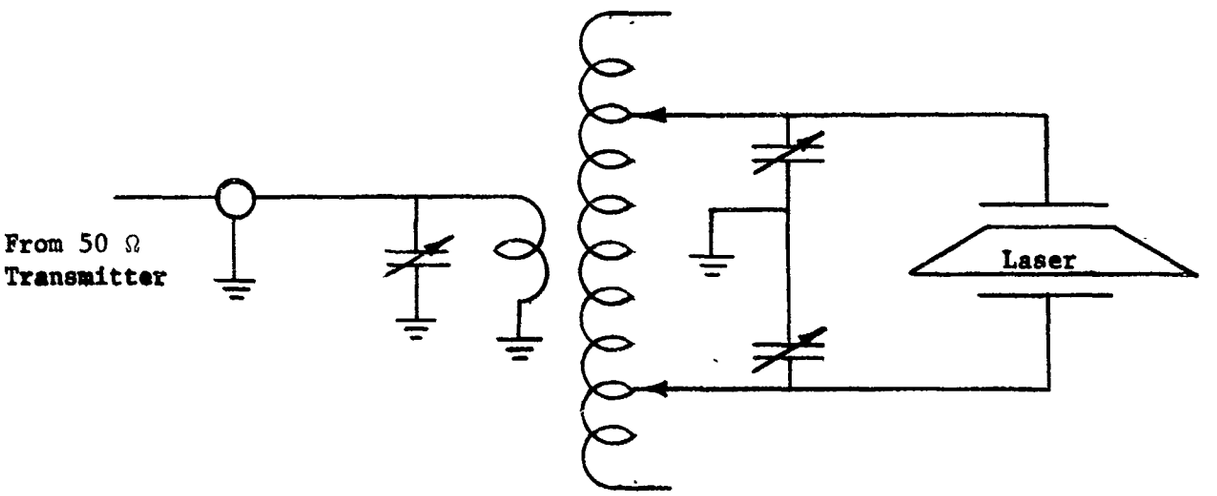

Figure 16. RF Matching Network.

Most of the tubes tested also had d.c. electrodes so that d.c. vs. RF power output data could be obtained. For most of the larger bore tubes with bore sizes greater than about 15 mm, the output powers and efficiencies were nearly identical for both types of excitation (8 watts typical multimode output with a 60 cm active length). However, as the bore size of the tubes was reduced, it became very difficult to obtain a uniform RF discharge across the transverse direction of the tube. The power output capability for the RF tube became quite poor while the d.c. discharge allowed continued high power operation. As will be seen in section 3.4, the small bore is very desirable if single-mode operation is necessary. For this reason RF excitation was abandoned in favor of d.c. excitation.

During the testing with RF excitation the following studies were made. Although not essential to the final results of the program, they are included here for completeness.

3.3.1 Parametric Studies

A short parametric study was made on the effects of gas mixture on the power output of the RF excited laser. A Brewster angle CO_2 laser with a bore diameter of 19 mm and an active length of 65 cm was operated with RF excitation. Strip electrodes were laid lengthwise along both sides of the cooling jacket. The electrode separation was approximately 32 mm. Several electrode widths from 1/8 inch to 1/2 inch were tried with very similar results in all cases. The laser was cooled by the low viscosity (1.5 centistokes) silicone fluid available from Dow Corning (DC 200). The wall temperature was maintained at about $20^{\circ}C$. The balanced line matching network described above was used to match the 50 ohm output of the 27 MHz oscillator to the tube impedance. Except when operating at the low power extremes of the transmitter, a VSWR of better than 1.2 was obtained. The maximum power output from the transmitter was 200 watts.

The laser utilized KCl Brewster windows polished flat to better than 1/10 λ at 10 microns. The optical cavity was formed by a 3 meter radius gold-coated mirror and an Irtran 2 multilayer dielectric mirror with a 15% transmission figure. The output mirror was anti-reflection-coated. The mirrors were mounted

on an optical bench rather than in a stable cavity for convenience, and the tube was allowed to run multimode.

Figure 17 is a graph of the output power from the laser as a function of gas pressure and composition. Only CO_2 and He mixtures were used; however, the addition of about 1 torr of N_2 increased the output by about 30% in most cases.

For the case of the 12 torr CO_2 pressure, helium was added beyond the point indicated on the graph in order to find the point at which oscillation would cease. At a total pressure of 40 torr, oscillation could no longer be detected, and the discharge in the tube was barely visible. At slightly higher pressures, the discharge could not be maintained. It is expected that higher pressures could be utilized with greater power supply capability.

In all cases, the output power was peaked by adjusting the input power. Generally at the lower helium pressures, the optimum input power would be about 60-100 watts, and as more helium was added the required input power rose until the maximum of 200 watts available was reached. It appears that higher output powers could be reached at higher pressures with greater power supply capability, although the efficiency may be degraded somewhat.

The data in the graph of Figure 17 was taken by adding the helium to the operating laser through a high vacuum valve from a helium reservoir. At the lower pressure values, the power output from the laser would immediately rise when more helium was added and then settle back to its equilibrium value after a few minutes of operation. However, at the higher pressure values, above about 6 torr of helium, the output of the laser would decrease by about 50% and then slowly come to its equilibrium value. At the highest pressures, the time constant for the process was about 1/2 hour. This very long time constant is attributed to the slow diffusion rate of the helium through the CO_2:He mixture.

As the pressure and gas mixture was changed in the laser discharge region, rather pronounced changes in the discharge characteristics were observed by

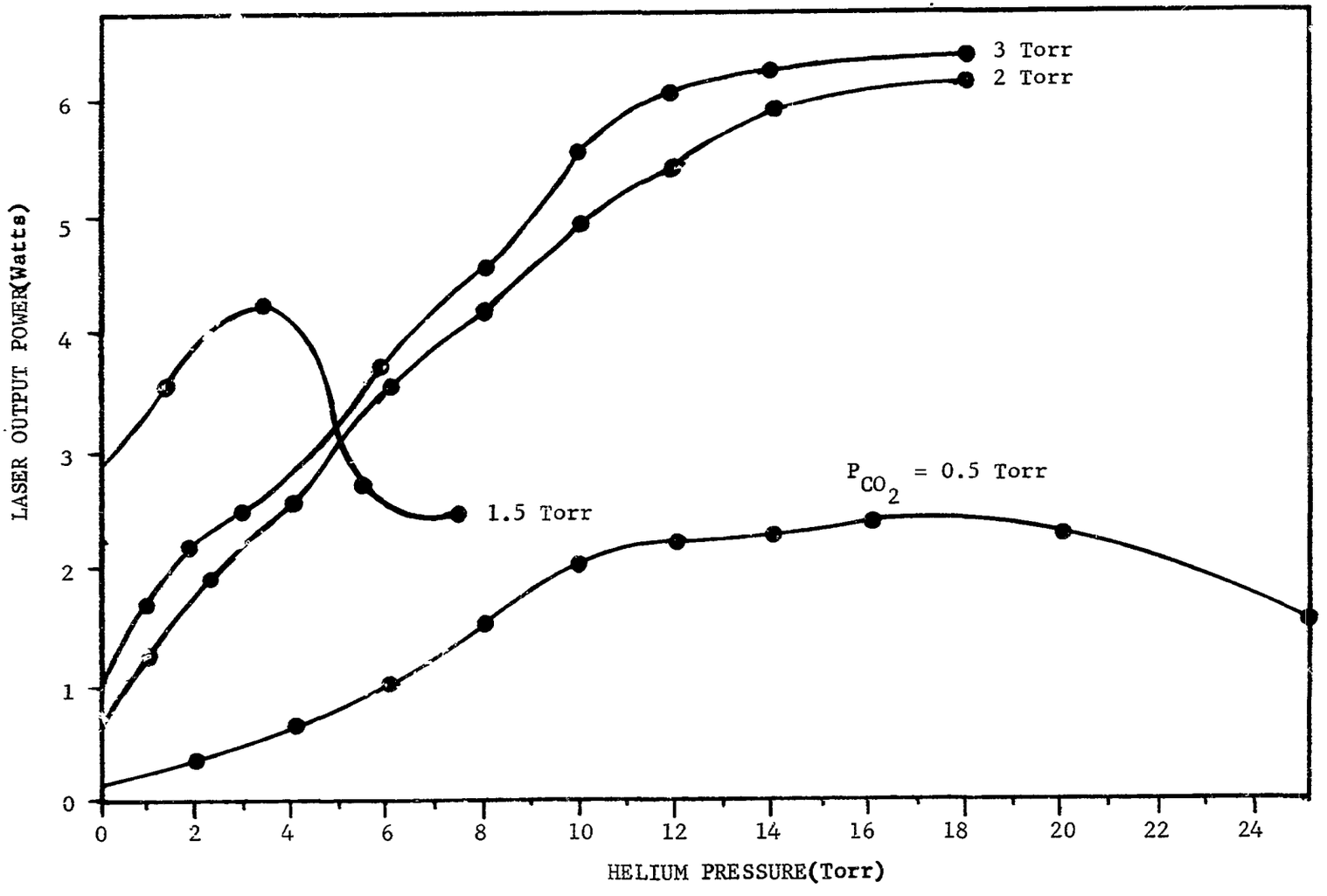

Figure 17. CO_2 Laser Output Power as a Function of Helium Partial Pressure for Various CO_2 Pressures (RF Excitation)

viewing the laser from the sides and down the bore. Generally, a bright discharge region could be observed just inside the laser walls opposite the strip electrodes. This bright discharge would fade to a uniform glow in the center of the tube. However, for some pressure fills, the discharge in the center would not remain uniform and intense discharges in local regions would be observed. This was especially apparent for the mixtures using the 1.5 torr CO_2 partial pressure and may account for the apparent anomolous power output characteristic at this pressure.

3.3.2 Window Coloring Effects

The Brewster window material we used in most of the test lasers was single crystal potassium chloride available from Harshaw Chemical. Normally these windows are quite transparent in the visible as well as the 10 micron region and appear clear to the eye. However, after operating on a laser tube after a period of time, the inside surface of the windows take on a bluish tint, and when the input power to the laser is high the windows can become very dark. A noticeable effect on the power output of the laser is also observed when the windows become dark blue.

The coloring effect is much more pronounced in the RF excited tubes than in the d.c. excited tubes. In a matter of only a few minutes after turn-on, the windows become noticeably colored when the RF lasers are operated at an RF power level of about 200 watts. Within an hour after turn-on, the laser windows are very dark, and the output power begins to decrease. Maximum power reductions of about 25% have been observed.

Clearing of the windows after the tube is turned off occurs, but the clearing is not complete, at least after a period of a few days. It appears that evacuating the tube allows some enhancement of the natural clearing rate. We also noticed that the rate of bluing was a function of the gas composition within the laser tube, and without the existence of CO_2 the bluing rate was very slow.

Although chemical effects on the inside surface of the KCl could not be ruled out, it appeared more likely that color centers (F centers) were being formed in the KCl due to some electrical or optical phenomena. The generation of color centers in the alkali halide crystals is well documented in the literature and can be caused in a variety of ways. The crystals may be colored by the introduction of suitable chemical impurities which themselves exhibit color. Also, introducing an excess of the cation, as by heating in the vapor of the alkali metal can result in the generation of color centers. When sodium chloride is processed in this fashion*, it exhibits a yellow color and potassium chloride exhibits a magenta color. It is also possible to color the crystals by x-ray and γ-ray radiation, neutron and electron bombardment and electrolysis.

Figure 18 shows the F band absorption for several alkali halides suitable for use as Brewster windows for 10.6 micron lasers. F bands introduced in KBr crystals should make the crystal appear light blue, due to its absorption in the red; NaCl should appear yellow, due to its absorption in the deep blue; and KCl should appear deep blue or magenta due to its absorption in the green and orange.

To verify that the coloring is the result of the formation of F centers, a discharge tube was fabricated with a KCl window on one end and a NaCl window on the other. The tube geometry is shown in Figure 19. Both windows were epoxied onto a Pyrex tube 3/4 inch in diameter and 30 inches long. No cooling jacket was used. The tube was cleaned internally by running a discharge in He only for a short period of time. The tube was then filled with a typical lasing mixture of CO_2, N_2, and He and operated for several hours. The KCl window turned a deep blue, and the NaCl window turned a light yellow color. After four hours of operation, the KCl window exhibited deep coloring throughout its volume with the intensity fading from the inside toward the outside face. The region outside the extended bore diameter of the discharge tube remained

*See C. Kittel, Introduction to Solid State Physics, 2nd Edition, pp. 492, (John Wiley & Sons, Inc., New York, 1956)

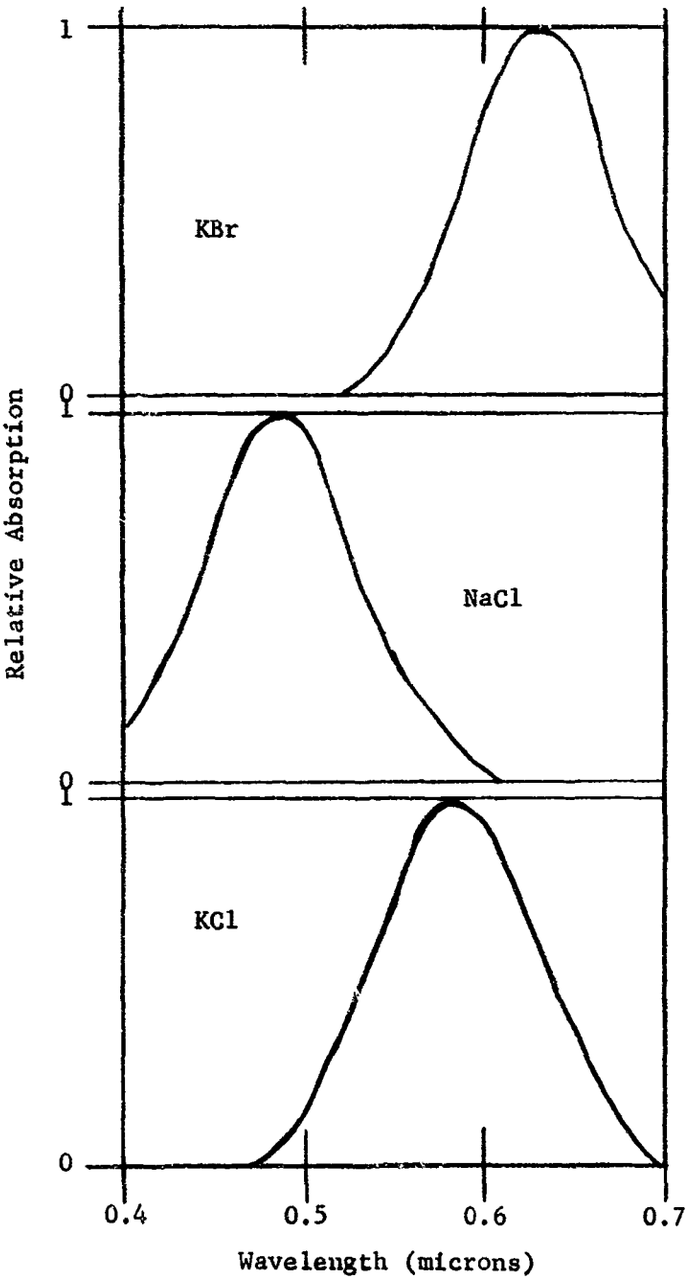

Figure 18. The F-Bands for Several Alkali Halides Useful as Brewster Angle Windows at 10.6 Microns. (Taken from Kittel)

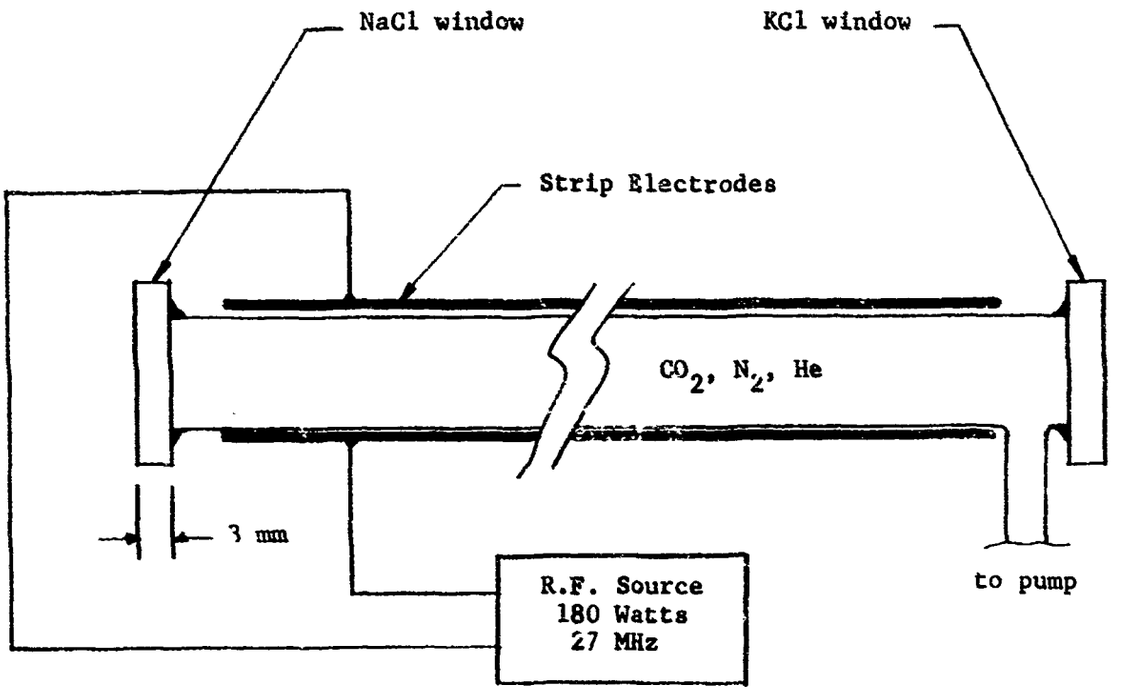

Figure 19. Experimental Demonstration of the Formation of F Bands in Alkali Halide Windows Used on CO_2 Laser Tubes

clear. The tube was dismantled and a transmission curve was run on the KCl window. The absorption matched well the expected absorption curve due to color centers. However, the NaCl crystal faded in color too rapidly to obtain an absorption curve with enough definition to correlate it with the expected curve. Also, the color intensity in the NaCl never did reach the intensity of the KCl crystal, and the coloring effect disappeared rather rapidly (several hours) compared to the KCl crystal.

We feel that the generation of color centers is caused by the absorption of ultraviolet radiation being emitted by the discharge. The transmission characteristics of NaCl to ultraviolet radiation is much better than for KCl, which may explain the color intensity difference between the two. Although we have not tested KBr, we would expect that the color intensity in this crystal will also be less than in KCl due to its better ultraviolet transmission characteristics.

To eliminate the possibility of electrical formation of the color centers, we fabricated a tube with long metal ends onto which the windows were attached. The tube was operated normally and with the ends grounded. No change in the rate of color formation was observed. Also, no effect was observed when high magnetic fields (approximately 400 gauss) were applied around the Brewster pipe.

As expected, with the formation of color centers, the coloring could be prevented or removed by the application of heat from infrared heat lamps to the windows. Thermal de-excitation and/or bleaching with light in the F absorption band of the crystal can return the crystal to its normal state. It was observed that temperatures in the range of $65^{\circ}C$ were required before the bluing effect in KCl could be completely eliminated.

Although the coloring effect is much more pronounced in RF tubes than in d.c. excited tubes, the coloring can be quite severe when the laser is operated at rather high d.c. current densities. However, during the latter stages of the program, after we had started using Xenon in most of the d.c. tubes, the coloring effect was no longer a problem. The lower excitation level within the

discharge caused by the addition of small amounts of Xenon gas had apparently reduced the intensity of emitted ultraviolet radiation to a low enough level that color centers were not formed to a significant degree.

3.3.3 Amplifier Gain Measurement

Before the decision was made to operate the amplifiers with d.c. excitation, single-pass gain measurements were made utilizing a 2-meter long RF-excited amplifier tube. The tube utilized Brewster windows on both ends.

Because of the 2-meter length of the tube, we had difficulty in breaking down the tube at the 27 MHz frequency we had used previously for the smaller oscillator tubes. Since the electrical length of the amplifier tube was a substantial fraction of a half wave at 27 MHz, we were not able to maintain a uniformly high voltage along the full length of the strip electrodes used. However, by reducing the driving frequency to 13 MHz and rebuilding the matching networks, we were able to drive the tube quite satisfactorily at a power level up to 500 watts input.

The bore diameter of the amplifier tube was 25 mm; however, only the central 10 mm diameter was used in the gain measurements. An oscillator which emitted up to 2.5 watts cw was used. The oscillator beam was passed through the amplifier tube, through a chopping wheel, a lens, and on to a gold-doped germanium detector. The gain was measured by turning the amplifier tube on and off.

The greatest gain figure observed for the tube was 1.67 for a 3 torr CO_2 and 8 torr He mixture. This corresponds to a gain figure of 28% per meter. At higher partial pressures of CO_2, the gain was reduced below this value. To establish whether any saturation effects were taking place, the oscillator power was reduced and the above gain measurements repeated. No saturation effects were observed.

The above gain figure can be compared to those obtained by Cheo and Cooper[5] for sealed-off, d.c. excited CO_2:He mixtures (40%/meter) and to those obtained

by Farrenq, et al.[6] for sealed-off, RF excited pure CO_2 (11%/meter) and CO_2:N_2 mixtures (22%/meter).

3.4 Laser Bore Size Effects

As mentioned in the previous section, several laser tubes were constructed to determine if there existed an optimum size tube for the case when RF excitation is used. All of the tubes had identical lengths of 75 cm with an active plasma length of about 60 cm. The bore sizes studied were 12, 19, and 27 mm in diameter in the plasma region. However, all the tubes were restricted to a 12 mm diameter optical size by an aperture, in order to compare their power output capabilities when operating in or near a single mode. The tubes were also equipped with internal cold cathode electrodes so that they could be operated dc.

Various combinations of gas pressures and mixtures were used to optimize the power output. The tests were also run with various input powers up to 200 watts.

The results of these tests indicated a very clear preference in favor of the smaller diameter laser tubes. The large bore tubes, although capable of producing greater total output power were severely limited when apertured down to where they would operate in a single mode. For the tests conducted, a 12 mm diameter aperture produced nearly a single-mode output as observed in a thermographic phosphor viewing screen of the type described by Bridges and Burkhardt[7]. As shown in Figure 20 the 27 mm diameter tube operated at the 1/2 watt level, the 19 mm tube at 1 watt, and the 12 mm tube at 2 watts. The 3% transmission multilayer dielectric output mirror used in these tests was not necessarily optimum for the tubes tested.

For the results obtained, a diameter dependent output for single mode or near single mode operation was seen to have a functional relationship of $\approx d^{-1.5}$, wnere d is the tube bore diameter. This functional relationship will, of course, not continue to hold when the tube size is reduced small enough that diffraction losses on the lowest order mode become large enough to severely limit the laser output power.

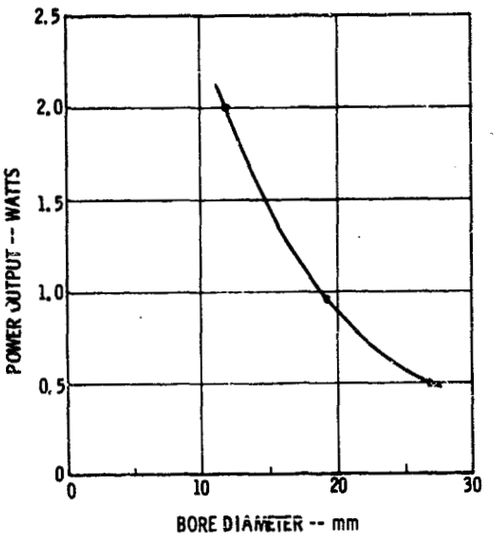

Figure 20. Near Single Mode Power Output as a Function of Bore Diameter

As mentioned in section 3.3, we were not able to obtain satisfactory results with the small bore tube when operated with RF excitation since a uniform discharge could not be obtained in the tube using parallel strip electrodes along the outside of the tube. This particular type of electrode geometry has proved most satisfactory for the larger bore tubes, but does not appear to be satisfactory for the smaller bore tubes. We were only able to obtain about 100 milliwatts from this tube using RF excitation, while the same tube would provide over 2 watts with d.c. excitation.

In later tests when the tubes were run in a stable cavity and with the aid of a gold-doped germanium detector, we found that a substantial amount of power was being emitted in other than the lowest order mode for the 12 mm bore tubes although this was not obvious from the output mode pattern. An aperture size of about 8 mm diameter was necessary to eliminate detectable beat frequencies between various modes. During these tests, various long-radius cavity configurations were used in which the non-output mirror was changed from a 2.15 meter to a 10 meter radius of curvature. The output mirror was flat.

In an attempt to obtain as much output power as possible in the lowest order mode, an 8 mm bore tube was constructed. Although this laser emitted between 3 and 5 watts, it did not do so in a pure single mode. The laser required a 6 mm aperture to eliminate the several beat frequencies observed. For the 8 mm bore tube, however, it was noticed that the beat notes were at a rather low frequency (1-2 MHz) compared to that which would be expected from resonator theory. Further investigation indicated that the smooth bore we were using in this tube was reflecting a substantial portion of the optical beam in the cavity, creating a very unusual optical cavity configuration. Succeeding tubes were constructed with a rippled bore to reduce wall reflections. With this arrangement, the beat frequencies were eliminated as long as the bore size remained smaller than 8 mm diameter. Bore sizes of 8 mm or larger did produce beat notes near the expected frequencies when the cavity resonance was set near the line center of the highest gain CO_2 transitions.

3.5 Frequency Stability Measurements

The auxiliary oscillator was used to heterodyne with the high power laser in a configuration shown in Figure 21. A portion of the beam from the high power laser was tapped off by the KCl window while the remainder was passed to a Coherent Radiation Laboratories Model 201 power meter. The power meter was calibrated by colorimetric techniques and found to be accurate to within 10%. The beams from the two lasers were combined by a 50-50 beam splitter using an Irtran 2 substrate, antireflection coated on one side with a high reflectivity dielectric coating on the other side. One leg from the beam splitter was passed through a Jarrell-Ash, 1/2-meter, grating monochromator (Model 82-000) while the other leg was focused on a Au:Ge detector through a KCl lens. The lens was used to increase the power on the detector element to about 100 mw.

The heterodyne beat note generated in the gold-doped germanium detector was observed on a spectrum analyzer (Hewlett-Packard Model No. 8551A), which is capable of displaying signals above 10 MHz. In most cases an upconverter was utilized (Hewlett-Packard Model No. K15-8551B) which allowed observation of the beat note below the 10 MHz limit to the basic spectrum analyzer. The stability levels were obtained by noticing the rate at which the laser frequency drifted on the spectrum analyzer screen or by the width of the beat note for short term stability figures.

Early stability tests resulted in stabilities of only approximately 1 or 2 MHz per second on both the long and short term. The major instabilities occurred at rates on the order of one to 10 cps, and was apparently caused by air turbulence between the Brewster-angle windows and the mirrors. At the time of these tests the window area was open to the rest of the cavity, although covers were placed over the top of the laser tubes, shielding them directly from the air conditioning and other air turbulence in the laboratory. However, after the Brewster-angle air path was covered by near hermetic seals, substantial increases in stability were obtained in the 1 to 10 cps region.

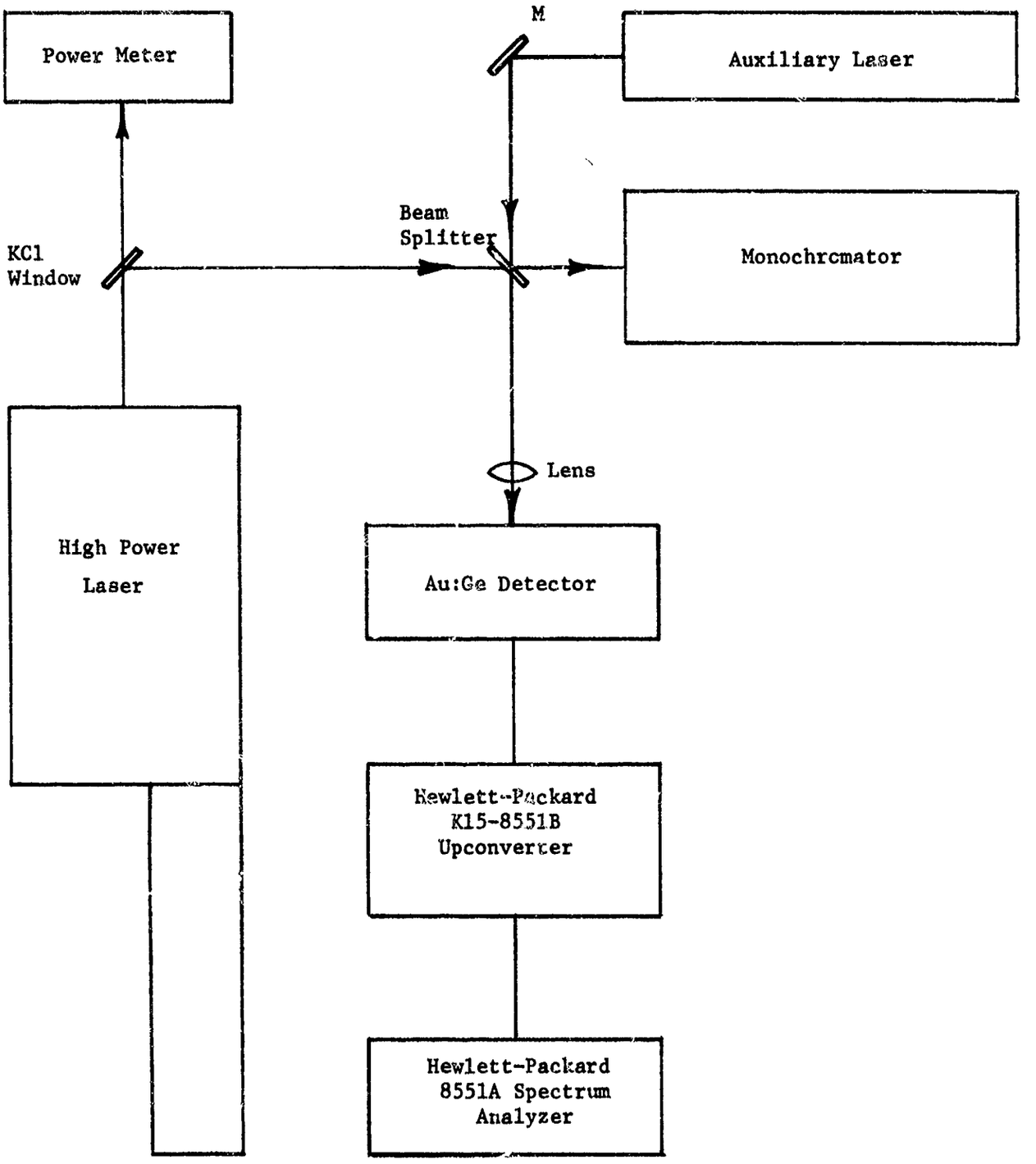

Figure 21. Physical Arrangement Used During Heterodyne Stability Tests.

The tests were run in a normal laboratory environment with equipment fans, pumps and air conditioning all operating. The lasers rested on standard laboratory benches rather than a stable granite table, and the only acoustic isolation used was that obtained from the outside laser enclosure.

Figure 22 shows three typical photographs of the heterodyne beat note at various degrees of stability. As the laser beat frequency drifted about due to thermal changes in the cavity, the beat note would drift in and out of view on the spectrum analyzer screen. Figure 22A shows two successive traces, indicating the beat frequency has drifted about 10 kHz during the time between successive sweeps (approximately 30 msec). The stability on an even shorter scale, characterized by the structure in each trace, appears to be near the resolution limit of the analyzer for this set of operating conditions (see Figure 23). In Figure 22B, three traces are captured within a total frequency span of about 24 kHz. The time period covering the three traces here is about 60 msec. Figure 22C shows the beat frequency during a time period when greater instabilities can be observed. The wider trace with more structure indicates greater short-term instabilities, although the drift is about the same as in the other photographs. Here the full excursion of the beat note, including the short-term instabilities is about 30 kHz for a time period of about 30 msec; however, in this case the line width during one of the traces is much greater than the resolution limit of the analyzer, as can be seen from the reference signal shown in Figure 23. The full width at half height for the broadest trace is about 16 kHz for a time period of roughly 3 msec.

Assuming that the lasers are acoustically statistically independent during the time periods involved, each laser can be considered to contribute equally to the beat note instability. The above figures then reduce to the following approximate instability range per laser

$$1.5 \text{ kHz} < \Delta f < 25 \text{ kHz}$$

for the time period of interest (10 msec). This corresponds to a fractional stability of

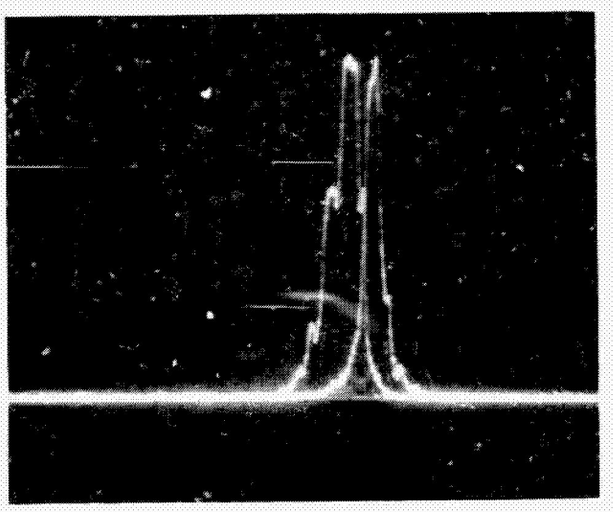

A

Vertical Scale: Linear
Horizontal Scale: 30 kHz/cm
Sweep Speed: 3 ms/cm
Exposure Time: 1/15 sec

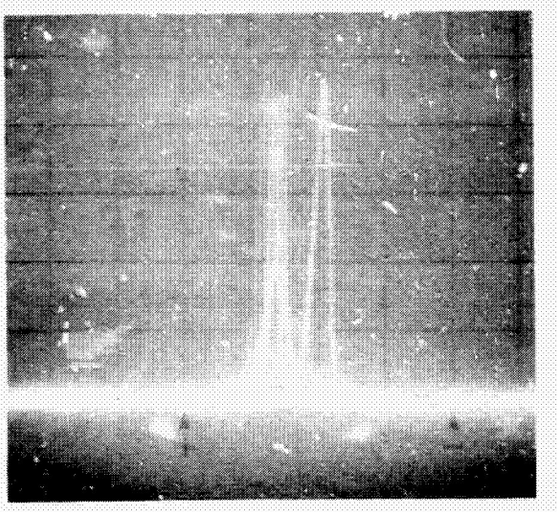

B

Vertical Scale: Linear
Horizontal Scale: 30 kHz/cm
Sweep Speed: 3 ms/cm
Exposure Time: 1/8 sec

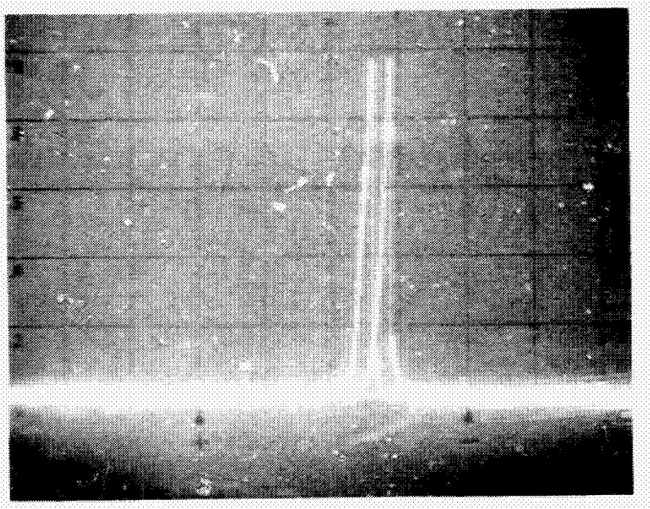

C

Vertical Scale: Linear
Horizontal Scale: 30 kHz/cm
Sweep Speed: 3 ms/cm
Exposure Time: 1/15 sec

Figure 22. Spectrum Analyzer Traces of Heterodyne Beat Frequency Between Two CO_2 Lasers Showing Short-Term Stability. Beat Frequency Occurs at about 1 MHz.

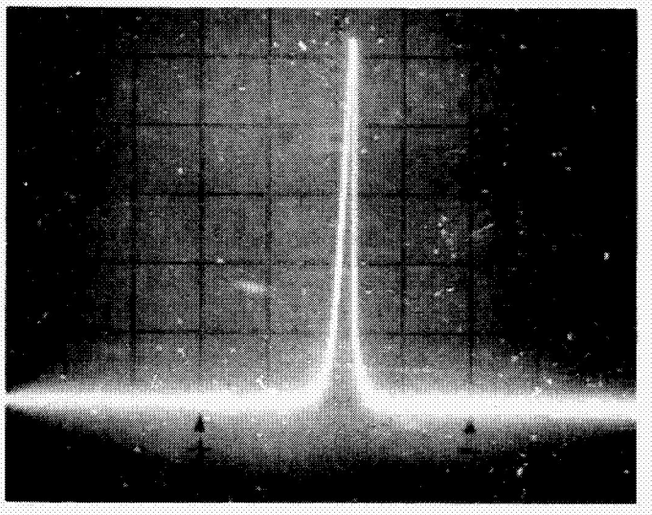

Vertical Scale: Linear
Horizontal Scale: 30 kHz/cm
Sweep Speed: 3 ms/cm

Figure 23. Spectrum Analyzer Display of 1 MHz RF Oscillator Showing Resolution Limit of Analyzer

$$5 \times 10^{-11} < \frac{\Delta f}{f} < 1 \times 10^{-9}$$

The above figures are, of course, strongly affected by the acoustical environment around the laser. Rapping on the table or loud whistling would spread the beat note to approximately 150 kHz. The long-term stability was quite adequate to maintain the laser output power constant to within about 5% on a single wavelength for an indefinite period of time. Once the laser structure was allowed to come to equilibrium, the frequency drift between the lasers stayed within a ±10 MHz band with a peak drift rate of about 100 kHz/sec. Also, once the proper operating conditions for the laser had been set, i.e., current, piezoelectric transducer voltage, water flow, etc., the laser could be turned off and on without changing wavelengths.

The sensitivity of the laser output frequency to amplitude changes of the discharge current was measured during the course of the experiments. By varying the applied voltage to the laser either manually or at 120 cps, the output frequency of the laser could be varied at the rate of about 750 kHz per milliamp change in the discharge current which corresponded in our case to about 200 volts change in the d.c. level of the applied voltage. This figure is slightly higher than that observed recently by H. Mocker[8] for lower pressure, flowing tubes. This effect may indeed be a prime contributor to the limits of the stability which we have observed since the supplies used with these lasers operate at about 15 kv and have a ripple figure only slightly better than .01%. Unfortunately, within the period of the program we were not able to perform more definitive tests on the effects of low ripple figures on laser frequency stability. It is also a possibility that any frequency instabilities caused by low level 60 or 120 cps modulation on the laser may not have been observed since the frequency of the lasers could be varying in phase.

From the measurements which were made, it appeared that the major single source of instability came from the acoustical environment. Apparently, the water cooling system on either laser was not the prime cause of vibrational effects. Shutting the water flow off for a short period did not measurably reduce the short-term instabilities. Earlier tests, however, did show that

the pump vibrations were coupling strongly into the laser structure. Since those early tests, an accumulator was added to the cooling system, the pump was better isolated, and 50 feet of rubber tubing was added between the pump and the laser head, all of which tend to reduce the coupling of vibrations from the pump.

3.6 Tilting Mount Experiment

In the intended application, the laser will be mounted on the side of a moving telescope and, while operating, will be tilted from a near horizontal position to a near vertical position. To determine the effects of tilting on the frequency stability and power stability of the laser, a test platform was made. A heterodyne check on stability was not attempted because of the unavailability of a suitably large and massive movable platform which could hold both lasers and associated equipment rigid to the required degree for heterodyne measurements.

Instead, a heavy plywood platform was constructed and hinged near one end to the edge of a work bench placed in the center of the laboratory. The high power laser, a power detector, a monochromator and associated optics were bolted to the platform. The laser was operated for about one hour to achieve thermal equilibrium before it was tilted. Because of the length of the laser and the ceiling limitations, we were not able to tilt the laser more than about 45^{o}.

With the laser tuned to the center of the 10.59 micron line, the laser was tilted several times to the 45^{o} limit. No change in output wavelength occurred. At each position, the laser frequency was retuned by the piezoelectric transducer power supply to as close to line center as could be detected by measuring the power transmission through the monochromator. The rounded-top pow output vs. frequency curve of this laser allowed an accuracy of about ±10 M to be obtained in seeking line center in this manner. In all positions the new transducer supply voltage coincided with the original voltage within the experimental error, concluding that the laser frequency did not change by more than ±10 MHz in tilting from 0 to 45^{o}.

A small change in power output, however, was observed. At the initial lift, the power output was reduced by about 10% at the 23 watt level. This change in power apparently was not due to a change in elevation but rather was due to a change in the mechanical forces acting on the laser as the plywood platform was stressed at the initial lift. As the laser was raised from 0 to 45^{o} a total maximum power variation of 5% was seen. The power variations observed were due primarily to detuning slightly the folding mirror structure used in the amplifier system rather than detuning of the laser oscillator since essentially no change in frequency was observed.

For these tests the back end of the amplifier was not tied down but was allowed to hang in a cantilever fashion without support. It is expected that when this unit is installed on the telescope with full mechanical support, the power variations with tilting will be substantially less than 5%.

4.0 NEW TECHNOLOGY DEVELOPMENTS

This program has been involved in the design and development of a new type of laser not previously available from any source. Therefore, the successful development of the laser can be considered an item of new technology. However, no new techniques or materials, not reported earlier out of other programs or sources, have been used in this development.

Section 6.0 summarizes the results of the program and briefly states the operating characteristics of the laser.

5.0 MATERIAL REPORT

This required section is presented for the purpose of disseminating information describing those tests, experiments, developments studies and other efforts of this laboratory on work relating to materials and their processing for use in fulfilling the technical requirements of this contract

One such effort was pursued during the first six months of the program involving the experimental determination of the shear modulus of elasticity of several low shear strength adhesives which fall into the soft epoxy and RTV class of materials. This effort was described in the first semi-annual materials report on this program.

No further efforts of this type have been pursued during the remainder of the program.

6.0 SUMMARY AND CONCLUSIONS

A sealed-off CO_2 laser has been developed which is capable of emitting a linearly polarized beam of infrared light at a single wavelength near 10.6 microns and at a power level of 38 watts. This output occurs in the TEM_{00q} mode and consists of a single frequency rather than a multitude of frequencies characteristic of most lasers. The main effort during the development of this laser centered in the area of improving the frequency stability of the laser. By careful mechanical and thermal design of the laser structure, short-term stabilities of better than 1 part in 10^{10} (3 kHz) were observed and long-term stabilities without electronic feedback of about $\pm$ 3 parts in 10^7 ($\pm$ 10 MHz) were obtained.

To achieve the requirements of very high short-term frequency stability simultaneously with high power, a master-oscillator-power-amplifier approach was taken. Total weight was also an important factor in the design since the laser is to be used in its final application on a rotating telescope.

The laser oscillator consisted of a Pyrex, Brewster angle laser tube using a 7 mm bore with an active length of 50 cm. The windows used on the tube were made from high-resistivity gallium arsenide. The tube was dc excited and used a Kovar cylindrical cathode and a tungsten pin anode. With a gas mixture of 1 torr Xe, 6 torr CO_2, 14 torr He the tube operated at about 10 kv at 10 ma and emitted about 5 watts of single-frequency power near 10.6 microns.

The laser tube was installed in a rigid channel-shaped cavity which also served to hold the laser mirrors. The mirrors were separated by four invar rods embedded in four corners of an aluminum channel. The mirror mounts as well as the rest of the structure were designed to reduce the effects of acoustical vibrations on the laser stability. To achieve the long-term stability the cavity structure was placed in an oven and the cavity temperature controlled to a $\pm$ .1° tolerance by a proportional temperature controller designed and constructed on this program.

The amplifier was designed to provide about 9 dB of gain through a folded structure with a total optical length of about 7 meters. The physical length of the amplifier is about 2 meters. The amplifier uses a bore of 18 mm diameter and operates at about 15 kv at 15 ma. It operates most efficiently with a mixture of 1/2 torr Xe, 3 torr CO_2 and 6 torr He.

During the course of the program several experiments and tests were performed to determine the optimum tube geometry and excitation mechanism. It was discovered that small bore tubes offer the greatest single mode power output and that dc excitation should be used. We were not able to generate a configuration in which RF excitation could be used on the small bore tubes and still maintain high output power.

The short-term frequency stability of the laser is greatly influenced by the acoustical environment of the laser. One of the most vulnerable areas of the laser is its path between the Brewster angle windows and the laser mirrors. Small changes in the air pressure in this region due primarily to acoustic vibrations can change the index of refraction of the air which in turn creates an effective change in the length of the cavity. Without tight covers surrounding this region, gross instabilities are observed.

Other major causes which may limit the stability of the laser are (1) vibrations introduced into the laser by the liquid cooling system; (2) airborne acoustic vibrations; and (3) low level amplitude modulation from the power supply due to imperfect filtering.

The laser was also tested on a tiltable platform and was found to remain operating on the same wavelength with no detectable gross frequency shift for the elevation angles between zero and 45° tested. Small power output variations were noticed, however, as the laser was tilted, but were attributed to bending and warping of the platform as the test was performed. It is not expected that the laser will have any noticeable power fluctuations when rigidly clamped to the telescope.

7.0 REFERENCES

1. A. E. Siegman, et al., "Laser Material (Spectroscopy)," Semi-Annual Report No. 2 (June 15, 1965 - December 15, 1965), Contract DA 28-043-AMC-00 446(E), U. S. Army Electronics Command, Fort Monmouth, New Jersey. M. L. Report No. 1401, Microwave Laboratory, W. W. Hansen Laboratory of Physics, Stanford University, California.

2. Handbook of Chemistry and Physics, Chemical Rubber Publishing Company, Cleveland, Ohio.

3. G. Hertzberg, Molecular Spectra and Molecular Structure I Spectra of Diatomic Molecules, D. Van Nostrand Company, Inc., New York, 1950.

4. P. O. Clark and J. Y Wada, "Characteristics of CO_2 - Xe-He Lasers," presented at the IEEE International Electron Devices Meeting, Washington, D.C., October 1967, paper 22.7.

5. P. K. Cheo and H. G. Cooper, "Gain Characteristics of CO_2 Laser Amplifiers at 10.6 Microns," IEEE J. Quantum Electronics, QE-3, p. 79 (February 1967).

6. R. Farrenq, et al., C. R. Academy of Sciencies, Paris, 261, pp. 2617-2620 (October 1965).

7. T. J. Bridges and E. G. Burkhardt, IEEE Journal of Quantum Electronics, QE-3, pp. 168, (April 1967).

8. H. Mocker, "Pressure and Current Dependent Shifts in the Frequency of Oscillation of the CO_2 Laser," Appl. Phys. Lett., 12, 20, (Jan. 1, 1968).